

---

# Diffusion Schrödinger Bridge Matching

---

**Yuyang Shi\***      **Valentin De Bortoli\***      **Andrew Campbell**      **Arnaud Doucet**  
University of Oxford      ENS ULM      University of Oxford      University of Oxford

## Abstract

Solving transport problems, i.e. finding a map transporting one given distribution to another, has numerous applications in machine learning. Novel mass transport methods motivated by generative modeling have recently been proposed, e.g. Denoising Diffusion Models (DDMs) and Flow Matching Models (FMMs) implement such a transport through a Stochastic Differential Equation (SDE) or an Ordinary Differential Equation (ODE). However, while it is desirable in many applications to approximate the deterministic dynamic Optimal Transport (OT) map which admits attractive properties, DDMs and FMMs are not guaranteed to provide transports close to the OT map. In contrast, Schrödinger bridges (SBs) compute stochastic dynamic mappings which recover entropy-regularized versions of OT. Unfortunately, existing numerical methods approximating SBs either scale poorly with dimension or accumulate errors across iterations. In this work, we introduce Iterative Markovian Fitting, a new methodology for solving SB problems, and Diffusion Schrödinger Bridge Matching (DSBM), a novel numerical algorithm for computing IMF iterates. DSBM significantly improves over previous SB numerics and recovers as special/limiting cases various recent transport methods. We demonstrate the performance of DSBM on a variety of problems.

## 1 Introduction

Mass transport problems are ubiquitous in machine learning (Peyré and Cuturi, 2019) with applications ranging from biology (Bunne et al., 2022) to shape correspondence (Feydy et al., 2017). For discrete measures, the Optimal Transport (OT) map can be computed exactly but is too computationally intensive. In a landmark paper, Cuturi (2013) has shown that an entropy-regularized version of OT can be computed efficiently using the Sinkhorn algorithm (Sinkhorn, 1967). This has enabled the implementation of OT techniques in a wide range of applications; see e.g. Benamou et al. (2015); Courty et al. (2017); Caron et al. (2020). However, while these techniques have been successful, they do not provide state-of-the-art performance for applications where high dimensional and/or continuous distributions are involved such as generative modeling.

Generative modeling is indeed a central machine learning transport problem which requires designing a deterministic or stochastic mapping transporting a reference “noise” distribution to the data distribution. For example, Generative Adversarial Networks (Goodfellow et al., 2014) define a static deterministic transport map while Denoising Diffusion Models (DDMs) (Song et al., 2021b; Ho et al., 2020) build a dynamic stochastic transport map by simulating a Stochastic Differential Equation (SDE) whose drift is learned using score matching techniques (Hyvärinen, 2005; Vincent, 2011). This denoising diffusion is the time-reversal of a forward “noising” diffusion initialized at the data distribution which transports the data approximately to a unit Gaussian distribution. The popularity and excellent performance of DDMs have motivated the development of novel Bridge Matching and Flow Matching Models which are dynamic transport techniques building stochastic maps using SDEs (Song et al., 2021a; Peluchetti, 2021; Liu, 2022; Albergo et al., 2023) or deterministic maps using ODEs (Albergo and Vanden-Eijnden, 2023; Heitz et al., 2023; Lipman et al., 2023; Liu et al., 2023b)

---

\*Equal contribution.

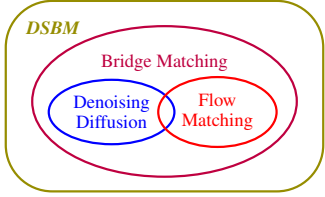


Figure 1: Relationship between DSBM and existing methods.

	Sets for alternating projections	Preserved properties
IPF	$\mathbb{P}_0 = \pi_0; \mathbb{P}_T = \pi_T$	$\mathcal{M}, \mathcal{R}(\mathbb{Q})$
IMF	$\mathcal{M}; \mathcal{R}(\mathbb{Q})$	$\mathbb{P}_0 = \pi_0, \mathbb{P}_T = \pi_T$

Table 1: Comparison between Iterative Markovian Fitting (IMF) and Iterative Proportional Fitting (IPF). The Schrödinger Bridge is the unique  $\mathbb{P}$  s.t.  $\mathbb{P}_0 = \pi_0, \mathbb{P}_T = \pi_T, \mathbb{P} \in \mathcal{M}, \mathbb{P} \in \mathcal{R}(\mathbb{Q})$  simultaneously by Proposition 5.  $\mathcal{M}$  is the space of (regular) Markov measures and  $\mathcal{R}(\mathbb{Q})$  the space of reciprocal measures of  $\mathbb{Q}$ .

whose drifts are approximated by solving a simple regression problem. These techniques not only do not require introducing a forward “noising” diffusion converging to a reference distribution, but are also more generally applicable than DDMs as they can approximate a transport map between any two distributions one can sample from by constructing “bridges” between them. Nonetheless, these dynamic transport maps are not necessarily close to the dynamic Optimal Transport (OT) map minimizing the Wasserstein-2 metric between the two distributions of interest, which is appealing for its many attractive theoretical properties (Peyré and Cuturi, 2019; Villani, 2009).

Unfortunately the dynamic OT map is intractable in realistic scenarios and, to the best of our knowledge, there is no available numerical techniques scaling to high dimensions. In contrast, the Schrödinger Bridge (SB) problem is a dynamic version of an entropy-regularized version of OT (Föllmer, 1988; Léonard, 2014b). The SB is the finite-time diffusion which is the closest in Kullback–Leibler divergence to a reference diffusion and admits as initial and terminal distributions the two distributions of interest. Numerous methods to approximate SBs numerically have been proposed, see e.g. (Bernton et al., 2019; Chen et al., 2016; Finlay et al., 2020; Caluya and Halder, 2021; Pavan et al., 2021), but these techniques tend to be restricted to low-dimensional settings. Recently novel techniques based on Iterative Proportional Fitting (IPF) (Fortet, 1940; Kullback, 1968; Rüschendorf and Thomsen, 1993), a continuous state-space extension of the Sinkhorn algorithm (Essid and Pavan, 2019), have been proposed in (De Bortoli et al., 2021; Vargas et al., 2021; Chen et al., 2022). In these contributions, the IPF iterates are approximated using diffusion-based ideas. These approaches scale better empirically than previous techniques but numerical errors tend to accumulate over iterations (Fernandes et al., 2021).

In this paper, our contributions are three-fold. First, we introduce Iterative Markovian Fitting (IMF), a new procedure to compute SBs which alternates between projecting on the space of Markov processes and projecting on the *reciprocal class* of the reference measure, i.e. the measures which have the same bridge as the reference measure of SB (Léonard et al., 2014). Contrary to IPF, the IMF iterates always preserve the initial and terminal distributions. The relationship between IPF and IMF is presented in Table 1. We establish various theoretical results for IMF. Second, we propose Diffusion Schrödinger Bridge Matching (DSBM), a novel algorithm approximating numerically the SB solution derived from IMF. This algorithm requires at each iteration to solve a simple regression problem in the spirit of (Peluchetti, 2021; Liu, 2022; Albergo and Vanden-Eijnden, 2023; Lipman et al., 2023; Liu et al., 2023b) and does not suffer from the time-discretization and the “forgetting” issues of previous techniques (De Bortoli et al., 2021; Vargas et al., 2021; Chen et al., 2022). We show that DSBM also sheds light on various recent dynamic deterministic and stochastic transport algorithms that it recovers as special/limiting cases. Finally, we demonstrate the performance of DSBM on a variety of transport tasks.

**Notations.** We denote by  $\mathcal{P}(\mathcal{C})$ , the space of *path measures*, i.e.  $\mathcal{P}(\mathcal{C}) = \mathcal{P}(C([0, T], \mathbb{R}^d))$  where  $T > 0$ . The subset of *Markov path measures* associated with an SDE of the form  $d\mathbf{X}_t = v_t(\mathbf{X}_t)dt + \sigma_t d\mathbf{B}_t$ , with  $\sigma, v$  locally Lipschitz, is denoted  $\mathcal{M}$ . For any  $\mathbb{Q} \in \mathcal{M}$ , the *reciprocal class* of  $\mathbb{Q}$  is denoted  $\mathcal{R}(\mathbb{Q})$ , see Definition 3. We also denote  $\mathbb{Q}_t$  its marginal distribution at time  $t$ ,  $\mathbb{Q}_{s,t}$  the joint distribution at times  $s$  and  $t$  and  $\mathbb{Q}_{s|t}$  the conditional distribution at time  $s$  given state at time  $t$ . Unless specified otherwise, all gradient operators  $\nabla$  are w.r.t. the variable  $x_t$  with time index  $t$ .

## 2 Dynamic Mass Transport Techniques

We begin by presenting Denoising Diffusion Models and Bridge Matching approaches. We then turn to their links with the Schrödinger Bridge problem.

## 2.1 Denoising Diffusion and Bridge Matching

Denoising Diffusion Models (Song et al., 2021b; Ho et al., 2020) are a popular class of generative models. We start with a forward noising process  $\mathbb{Q} \in \mathcal{M}$  associated with the SDE,  $d\mathbf{X}_t = -\frac{1}{2}\mathbf{X}_t dt + d\mathbf{B}_t$ , on the time-interval  $[0, T]$ , where  $\mathbf{X}_0 \in \mathbb{R}^d$  is drawn from the data distribution  $\pi_0$  and  $(\mathbf{B}_t)_{t \in [0, T]}$  is a multivariate standard Brownian motion. This diffusion, known as the Ornstein-Uhlenbeck (OU) process<sup>2</sup>, converges towards the standard multivariate Gaussian distribution  $\mathcal{N}(0, \text{Id})$  as  $T \rightarrow \infty$ . A generative model is given by the *time-reversal*  $(\mathbf{Y}_t)_{t \in [0, T]} = (\mathbf{X}_{T-t})_{t \in [0, T]}$ , where  $\mathbf{Y}_0 \sim \mathbb{Q}_T$  and  $d\mathbf{Y}_t = \{\frac{1}{2}\mathbf{Y}_t + \nabla \log \mathbb{Q}_{T-t}(\mathbf{Y}_t)\}dt + d\mathbf{B}_t$  (Anderson, 1982; Haussmann and Pardoux, 1986) for  $\mathbb{Q}_t = \text{Law}(\mathbf{X}_t)$ . In practice,  $(\mathbf{Y}_t)_{t \in [0, T]}$  is initialized with  $\mathbf{Y}_0 \sim \pi_T = \mathcal{N}(0, \text{Id})$  and the *Stein score*  $\nabla \log \mathbb{Q}_t(x_t) = \mathbb{E}_{\mathbb{Q}_{0|t}}[\nabla \log \mathbb{Q}_{t|0}(\mathbf{X}_t | \mathbf{X}_0) | \mathbf{X}_t = x_t]$  is approximated by a neural network  $s_\theta(t, x_t)$  whose parameters are obtained by minimizing the regression objective  $\mathbb{E}_{\mathbb{Q}_{0,t}}[\|\nabla \log \mathbb{Q}_{t|0}(\mathbf{X}_t | \mathbf{X}_0) - s_\theta(t, \mathbf{X}_t)\|^2]$ , see Vincent (2011).

An alternative to considering the time-reversal of a forward noising process is to build bridges between the two boundary distributions and learn a *mimicking* diffusion process. This approach generalizes DDMs and allows for more flexible choices of sampling processes. We call this framework *Bridge Matching* and adopt a presentation similar to Peluchetti (2021); Liu et al. (2022b), where  $\pi_T$  is the data distribution<sup>3</sup>. We denote  $\mathbb{Q} \in \mathcal{M}$  the distribution of the following process

$$d\mathbf{X}_t = f_t(\mathbf{X}_t)dt + \sigma_t d\mathbf{B}_t, \quad \mathbf{X}_0 \sim \mathbb{Q}_0. \quad (1)$$

Consider now the law of this process pinned down at an initial and terminal point  $x_0, x_T$ , denoted  $\mathbb{Q}_{|0,T}(\cdot | x_0, x_T)$ . Under mild assumptions, the *conditioned* process  $\mathbb{Q}_{|0,T}(\cdot | x_0, x_T)$  is associated with the SDE

$$d\mathbf{X}_t^{0,T} = \{f_t(\mathbf{X}_t^{0,T}) + \sigma_t^2 \nabla \log \mathbb{Q}_{T|t}(x_T | \mathbf{X}_t^{0,T})\}dt + \sigma_t d\mathbf{B}_t, \quad \mathbf{X}_0^{0,T} = x_0, \quad (2)$$

which satisfies  $\mathbf{X}_T^{0,T} = x_T$  by using results from the Doob *h*-transform theory (Rogers and Williams, 2000). Next we define an independent coupling  $\Pi_{0,T} = \pi_0 \otimes \pi_T$  between  $\pi_0, \pi_T$ , and let  $\Pi = \int \mathbb{Q}_{|0,T} d\Pi_{0,T}$ . This path measure  $\Pi$  is a *mixture of bridges*, where the bridge measure  $\mathbb{Q}_{|0,T}$  is integrated at its end points over the coupling  $\Pi_{0,T}$ . Note that while the bridge  $\mathbb{Q}_{|0,T}$  is Markov, the mixture  $\Pi$  is usually not a Markov process. We aim to find a Markov diffusion  $(\mathbf{Y}_t)_{t \in [0, T]}$  defined by  $d\mathbf{Y}_t = \{f_t(\mathbf{Y}_t) + v_t(\mathbf{Y}_t)\}dt + \sigma_t d\mathbf{B}_t$ ,  $\mathbf{Y}_0 \sim \pi_0$ , which admits the same marginals as  $\Pi$ ; i.e. for any  $t \in [0, T]$ ,  $\mathbf{Y}_t \sim \Pi_t$ , and in particular  $\mathbf{Y}_T \sim \pi_T$ . For such a velocity field  $v_t$ , a generative model for sampling data distribution  $\pi_T$  is given by (i) sampling  $\mathbf{Y}_0 \sim \pi_0 = \mathcal{N}(0, \text{Id})$ , (ii) simulating  $d\mathbf{Y}_t = \{f_t(\mathbf{Y}_t) + v_t(\mathbf{Y}_t)\}dt + \sigma_t d\mathbf{B}_t$ . It can be shown that indeed  $\mathbf{Y}_t \sim \Pi_t$  holds true for  $v_t^*(x_t) = \sigma_t^2 \mathbb{E}_{\Pi_{T|t}}[\nabla \log \mathbb{Q}_{T|t}(\mathbf{X}_T | \mathbf{X}_t) | \mathbf{X}_t = x_t]$ . We present the theory behind this idea more formally using Markovian projections in Section 3.1. In practice, we do not have access to  $v_t^*$  and it is learned using neural networks with a regression loss

$$\mathbb{E}_{\Pi_{t,T}}[\|\sigma_t^2 \nabla \log \mathbb{Q}_{T|t}(\mathbf{X}_T | \mathbf{X}_t) - v_\theta(t, \mathbf{X}_t)\|^2].$$

In the case where  $f_t = 0$  and  $\sigma_t = \sigma$ ,  $\mathbb{Q}_{|0,T}$  is a *Brownian Bridge* and we have

$$\mathbf{X}_t^{0,T} = \frac{t}{T}x_T + (1 - \frac{t}{T})x_0 + \sigma_t(\mathbf{B}_t - \frac{t}{T}\mathbf{B}_T), \quad d\mathbf{X}_t^{0,T} = \{(x_T - \mathbf{X}_t^{0,T})/(T-t)\}dt + \sigma_t d\mathbf{B}_t, \quad (3)$$

with  $(\mathbf{B}_t - \frac{t}{T}\mathbf{B}_T) \sim \mathcal{N}(0, t(1 - \frac{t}{T}) \text{Id})$ . The regression loss associated with (3) is given by

$$\mathbb{E}_{\Pi_{t,T}}[\|(\mathbf{X}_T - \mathbf{X}_t)/(T-t) - v_\theta(t, \mathbf{X}_t)\|^2]. \quad (4)$$

Letting  $\sigma \rightarrow 0$ , we recover Flow Matching Models<sup>4</sup>. More generally, while the Markovian projection introduced in Section 3 and the new DSBM methodology presented in Section 4 are stated in a *stochastic* context, since they rely on stochastic tools such as the Girsanov theorem, deterministic counterparts can be obtained by letting  $\sigma \rightarrow 0$ .

<sup>2</sup>This is referred to as variance preserving SDE (VPSDE) in Song et al. (2021b). For ease of presentation, we omit the time rescaling.

<sup>3</sup>To keep notations consistent with existing works,  $\pi_0$  is the data distribution in the context of DDM and SB, whereas  $\pi_T$  is the data distribution in FMM. However, both SB and FMM allow transfer between general distributions  $\pi_0, \pi_T$ , so this distinction is not important.

<sup>4</sup>We clarify this further as well as the relationship between different Flow Matching Models in Appendix A.

## 2.2 Optimal Transport and Schrödinger Bridges

The static optimal transport (OT) map is defined as the coupling between  $\pi_0$  and  $\pi_T$  minimizing the Wasserstein-2 metric, i.e.

$$\Pi_{0,T}^{\text{OT}} = \operatorname{argmin}_{\Pi_{0,T}} \{ \mathbb{E}_{\Pi_{0,T}} [ \| \mathbf{X}_0 - \mathbf{X}_T \|^2 ] : \Pi_0 = \pi_0, \Pi_T = \pi_T \},$$

i.e. it is the probability coupling with marginals  $\pi_0$  and  $\pi_T$  minimizing the expected square Euclidean distance between  $\mathbf{X}_0$  and  $\mathbf{X}_T$ . A famous result by [Benamou and Brenier \(2000\)](#) is that, under mild assumptions on  $\pi_0, \pi_T$ , the OT map can be obtained by solving a *dynamic* transport problem

$$v_{\text{OT}} = \operatorname{argmin}_v \{ \int_0^T \mathbb{E}_{\mathbb{P}_t} [ \| v(t, \mathbf{X}_t) \|^2 ] dt : d\mathbf{X}_t = v(t, \mathbf{X}_t) dt, \mathbb{P}_0 = \pi_0, \mathbb{P}_T = \pi_T \}, \quad (5)$$

for  $\mathbb{P}_t = \text{Law}(\mathbf{X}_t)$ ; i.e.  $v_{\text{OT}}$  is the velocity field minimizing the time integral of the kinetic energy among all vector fields such that the ODE initialized at  $\mathbf{X}_0 \sim \pi_0$  yields  $\mathbf{X}_T \sim \pi_T$ . The OT map is then obtained by sampling  $\mathbf{X}_0 \sim \pi_0$  followed by  $d\mathbf{X}_t = v_{\text{OT}}(t, \mathbf{X}_t) dt$ . The joint samples at the initial and final times satisfy  $(\mathbf{X}_0, \mathbf{X}_T) \sim \Pi_{0,T}^{\text{OT}}$ .

The Schrödinger Bridge (SB) problem ([Schrödinger, 1932](#)) is a dynamic version of an Entropy-regularized Optimal Transport (EOT) problem ([Mikami and Thieullen, 2008](#); [Léonard, 2014b](#); [Chen et al., 2021](#)). It consists in finding a path measure  $\mathbb{P}^{\text{SB}} \in \mathcal{P}(\mathcal{C})$  such that

$$\mathbb{P}^{\text{SB}} = \operatorname{argmin}_{\mathbb{P}} \{ \text{KL}(\mathbb{P} | \mathbb{Q}) : \mathbb{P}_0 = \pi_0, \mathbb{P}_T = \pi_T \}, \quad (6)$$

where  $\mathbb{Q} \in \mathcal{P}(\mathcal{C})$  is a reference path measure. In what follows, we consider  $\mathbb{Q}$  defined by the diffusion process (1) which is Markov, and without loss of generality, we assume  $\mathbb{Q}_0 = \pi_0$ . Hence  $\mathbb{P}^{\text{SB}}$  is the path measure closest to  $\mathbb{Q}$  in terms of Kullback–Leibler divergence which satisfies the initial and terminal constraints  $\mathbb{P}_0^{\text{SB}} = \pi_0$  and  $\mathbb{P}_T^{\text{SB}} = \pi_T$ . Note that we also have  $\mathbb{P}^{\text{SB}} = \int \mathbb{Q}_{|0,T} d\Pi_{0,T}^{\text{SB}}$  where  $\Pi_{0,T}^{\text{SB}} = \operatorname{argmin}_{\Pi_{0,T}} \{ \text{KL}(\Pi_{0,T} | \mathbb{Q}_{0,T}) : \Pi_0 = \pi_0, \Pi_T = \pi_T \}$  is the solution of the *static* SB problem ([Léonard, 2014b](#)). In particular, for  $\mathbb{Q}$  a multivariate Brownian of standard deviation  $\sigma$ ,

$$\Pi_{0,T}^{\text{SB}} = \operatorname{argmin}_{\Pi_{0,T}} \{ \mathbb{E}_{\Pi_{0,T}} [ \| \mathbf{X}_0 - \mathbf{X}_T \|^2 - 2\sigma^2 T \text{H}(\Pi_{0,T}) ] : \Pi_0 = \pi_0, \Pi_T = \pi_T \},$$

where  $\text{H}(\mu) = - \int \log(d\mu/d\text{Leb}) d\mu$  denotes the entropy, i.e.  $\Pi_{0,T}^{\text{SB}}$  is an entropy-regularized OT plan. This transport can also be obtained theoretically by solving the following problem related to (5)

$$v_{\text{SB}} = \operatorname{argmin}_v \{ \int_0^T \mathbb{E}_{\mathbb{P}_t} [ \| v(t, \mathbf{X}_t) \|^2 ] dt : d\mathbf{X}_t = v(t, \mathbf{X}_t) dt + \sigma dB_t, \mathbb{P}_0 = \pi_0, \mathbb{P}_T = \pi_T \}.$$

Then the SDE with drift  $v_{\text{SB}}$  initialized with  $\mathbf{X}_0 \sim \pi_0$  is such that  $(\mathbf{X}_0, \mathbf{X}_T) \sim \Pi_{0,T}^{\text{SB}}$ . A common approach to solve (6) is the Iterative Proportional Fitting (IPF) method ([Fortet, 1940](#); [Kullback, 1968](#); [Rüschendorf, 1995](#)) defining a sequence of path measures  $(\mathbb{P}^n)_{n \in \mathbb{N}}$  where

$$\mathbb{P}^{2n+1} = \operatorname{argmin}_{\mathbb{P}} \{ \text{KL}(\mathbb{P} | \mathbb{P}^{2n}) : \mathbb{P}_T = \pi_T \}, \quad \mathbb{P}^{2n+2} = \operatorname{argmin}_{\mathbb{P}} \{ \text{KL}(\mathbb{P} | \mathbb{P}^{2n+1}) : \mathbb{P}_0 = \pi_0 \}, \quad (7)$$

with initialization  $\mathbb{P}^0 = \mathbb{Q}$ . This procedure alternates between projections on the set of path measures with given initial distribution  $\pi_0$  and the set of path measures with given terminal distribution  $\pi_T$ . It can be shown ([De Bortoli et al., 2021](#)) that the distributions  $(\mathbb{P}^n)_{n \in \mathbb{N}}$  are associated with diffusions and that for any  $n \in \mathbb{N}$ ,  $\mathbb{P}^{2n+1}$  is the time-reversal of  $\mathbb{P}^{2n}$  with initialization  $\pi_T$  and  $\mathbb{P}^{2n+2}$  is the time-reversal of  $\mathbb{P}^{2n+1}$  with initialization  $\pi_0$ . Leveraging this property, [De Bortoli et al. \(2021\)](#) propose Diffusion Schrödinger Bridge (DSB), an algorithm which learns the time-reversals iteratively using neural networks. In particular, DDMs can be seen as the first iteration of DSB.

## 3 Iterative Markovian Fitting

### 3.1 Markovian Projection and Reciprocal Projection

**Markovian Projection.** *Markovian projection* is a key ingredient in our methodology and in the Bridge Matching framework. This concept was introduced multiple times in the literature ([Gyöngy, 1986](#); [Peluchetti, 2021](#); [Liu et al., 2022b](#)). In particular, we focus on Markovian projection of path measures given by a mixture of bridges  $\Pi = \int \mathbb{Q}_{|0,T} d\Pi_{0,T} \in \mathcal{P}(\mathcal{C})$ .

**Definition 1.** Assume that  $\mathbb{Q}$  is given by (1) and that for any  $(x_0, x_T) \in \mathbb{R}^d$ ,  $\mathbb{Q}_{|0,T}(\cdot|x_0, x_T)$  is associated with  $(\mathbf{X}_t^{0,T})_{t \in [0,T]}$  given by  $d\mathbf{X}_t^{0,T} = \{f_t(\mathbf{X}_t^{0,T}) + \sigma_t^2 \nabla \log \mathbb{Q}_{T|t}(x_T|\mathbf{X}_t^{0,T})\}dt + \sigma_t d\mathbf{B}_t$ , with  $\sigma : [0, T] \rightarrow (0, +\infty)$ . Then, when it is well-defined, we introduce the Markovian projection of  $\Pi$ ,  $\mathbb{M}^* = \text{proj}_{\mathcal{M}}(\Pi) \in \mathcal{M}$ , associated with the SDE

$$d\mathbf{X}_t^* = \{f_t(\mathbf{X}_t^*) + v_t^*(\mathbf{X}_t^*)\}dt + \sigma_t d\mathbf{B}_t, \quad v_t^*(x_t) = \sigma_t^2 \mathbb{E}_{\Pi_{T|t}}[\nabla \log \mathbb{Q}_{T|t}(\mathbf{X}_T|\mathbf{X}_t) | \mathbf{X}_t = x_t].$$

Note that in our definition  $\sigma_t > 0$  so  $\nabla \log \mathbb{Q}_{T|t}(x_T|x_t)$  is well-defined, but Flow Matching can be recovered as the *deterministic* case in the limit  $\sigma_t = \sigma \rightarrow 0$ . For simplicity, we also assume that  $\mathbb{Q}$  is Markov but Definition 1 can be extended to the non-Markovian setting. We use the term *Markovian projection* since  $\mathbb{M}^*$  is Markovian (as it is given by a Itô diffusion), while  $\Pi$  might not be. In the following proposition, we show that the Markovian projection is indeed a projection for the *reverse* Kullback–Leibler divergence, and that it preserves marginals of  $\Pi_t$ .

**Proposition 2.** Assume that  $\sigma_t > 0$ . Let  $\mathbb{M}^* = \text{proj}_{\mathcal{M}}(\Pi)$ . Then, under mild assumptions, we have

$$\mathbb{M}^* = \text{argmin}_{\mathbb{M}} \{\text{KL}(\Pi|\mathbb{M}) : \mathbb{M} \in \mathcal{M}\},$$

$$\text{KL}(\Pi|\mathbb{M}^*) = \frac{1}{2} \int_0^T \mathbb{E}_{\Pi_{0,t}} [\|\sigma_t^2 \mathbb{E}_{\Pi_{T|0,t}}[\nabla \log \mathbb{Q}_{T|t}(\mathbf{X}_T|\mathbf{X}_t) | \mathbf{X}_0, \mathbf{X}_t] - v_t^*(\mathbf{X}_t)\|^2] / \sigma_t^2 dt.$$

In addition, we have that for any  $t \in [0, T]$ ,  $\mathbb{M}_t^* = \Pi_t$ . In particular,  $\mathbb{M}_T^* = \Pi_T$ .

**Reciprocal Projection.** While the Markovian projection  $\text{proj}_{\mathcal{M}}$  ensures that the obtained measure is Markov, the associated *bridge* measure is not preserved in general, i.e.  $\text{proj}_{\mathcal{M}}(\Pi)_{|0,T} \neq \Pi_{|0,T} = \mathbb{Q}_{|0,T}$ . Measures with same bridge as  $\mathbb{Q}$  are said to be in its *reciprocal class* (Léonard et al., 2014).

**Definition 3.**  $\Pi \in \mathcal{P}(\mathcal{C})$  is in the reciprocal class of  $\mathbb{Q} \in \mathcal{M}$  if  $\Pi = \int \mathbb{Q}_{|0,T} d\Pi_{0,T}$ . We denote by  $\mathcal{R}(\mathbb{Q})$  the reciprocal class of  $\mathbb{Q}$ . We define the reciprocal projection of  $\mathbb{P} \in \mathcal{P}(\mathcal{C})$  as  $\Pi^* = \text{proj}_{\mathcal{R}(\mathbb{Q})}(\mathbb{P}) = \int \mathbb{Q}_{|0,T} d\Pi_{0,T}$ .

Similarly to Proposition 2, we have the following result, which justifies the term reciprocal projection.

**Proposition 4.** Let  $\mathbb{P} \in \mathcal{P}(\mathcal{C})$ ,  $\Pi^* = \text{proj}_{\mathcal{R}(\mathbb{Q})}(\mathbb{P})$ . Then,  $\Pi^* = \text{argmin}_{\Pi} \{\text{KL}(\mathbb{P}|\Pi) : \Pi \in \mathcal{R}(\mathbb{Q})\}$ .

The reciprocal projection  $\Pi^*$  of a Markov path measure  $\mathbb{M}$  does not preserve the Markov property in general. In fact, the Schrödinger Bridge is the *unique* path measure which satisfies the initial and terminal conditions, is Markov and is in the reciprocal class of  $\mathbb{Q}$ , see (Léonard, 2014b). The following proposition makes this link explicit.

**Proposition 5.** Let  $\mathbb{P}$  be a Markov measure in the reciprocal class of  $\mathbb{Q}$  such that  $\mathbb{P}_0 = \pi_0$ ,  $\mathbb{P}_T = \pi_T$ . Then, under assumptions on  $\mathbb{Q}$ ,  $\pi_0$  and  $\pi_T$ ,  $\mathbb{P}$  is unique and is equal to the Schrödinger Bridge  $\mathbb{P}^{\text{SB}}$ .

### 3.2 Iterative Markovian Fitting

Based on Proposition 5, we propose a novel methodology called *Iterative Markovian Fitting* (IMF) to solve Schrödinger Bridges. We consider a sequence  $(\mathbb{P}^n)_{n \in \mathbb{N}}$  such that

$$\mathbb{P}^{2n+1} = \text{proj}_{\mathcal{M}}(\mathbb{P}^{2n}), \quad \mathbb{P}^{2n+2} = \text{proj}_{\mathcal{R}(\mathbb{Q})}(\mathbb{P}^{2n+1}), \quad (8)$$

with  $\mathbb{P}^0$  such that  $\mathbb{P}_0^0 = \pi_0$ ,  $\mathbb{P}_T^0 = \pi_T$  and  $\mathbb{P}^0 \in \mathcal{R}(\mathbb{Q})$ . These updates correspond to alternatively performing Markovian projections and reciprocal projections. Note that for any  $n \in \mathbb{N}$ ,  $\mathbb{P}^{2n+1}$  is Markov and  $\mathbb{P}^{2n}$  is in the reciprocal class of  $\mathbb{Q}$ .

Combining Proposition 2 and Definition 3, we get that for any  $n \in \mathbb{N}$ ,  $\mathbb{P}_0^n = \pi_0$  and  $\mathbb{P}_T^n = \pi_T$ . This last property is in contrast with the sequence generated by the IPF algorithm (7) for which the marginals at the initial and final times are *not* preserved. Here the marginals are preserved, but we iteratively project on the set of Markov measures and the reciprocal class of  $\mathbb{Q}$ . We highlight this duality between IPF (7) and IMF (8) in Table 1.

We conclude this section with a preliminary theoretical analysis of IMF. First, we start by showing a Pythagorean theorem for both the Markovian projection and the reciprocal projection.

**Lemma 6.** Under mild assumptions, if  $\mathbb{M} \in \mathcal{M}$ ,  $\Pi \in \mathcal{R}(\mathbb{Q})$  and  $\text{KL}(\Pi|\mathbb{M}) < +\infty$ , we have

$$\text{KL}(\Pi|\mathbb{M}) = \text{KL}(\Pi|\text{proj}_{\mathcal{M}}(\Pi)) + \text{KL}(\text{proj}_{\mathcal{M}}(\Pi)|\mathbb{M}).$$

If  $\text{KL}(\mathbb{M}|\Pi) < +\infty$ , we have

$$\text{KL}(\mathbb{M}|\Pi) = \text{KL}(\mathbb{M}|\text{proj}_{\mathcal{R}(\mathbb{Q})}(\mathbb{M})) + \text{KL}(\text{proj}_{\mathcal{R}(\mathbb{Q})}(\mathbb{M})|\Pi).$$

This result should be compared with the information geometry result of (Csiszár, 1975, Theorem 2.2), which states that if  $\mathcal{C}$  is a convex set and  $\mathbb{P} \in \mathcal{C}$ , then under mild conditions,  $\text{KL}(\mathbb{P}|\mathbb{Q}) = \text{KL}(\mathbb{P}|\text{proj}_{\mathcal{C}}(\mathbb{Q})) + \text{KL}(\text{proj}_{\mathcal{C}}(\mathbb{Q})|\mathbb{Q})$ , where  $\text{proj}_{\mathcal{C}}(\mathbb{Q}) = \text{argmin}_{\mathbb{P} \in \mathcal{C}} \{\text{KL}(\mathbb{P}|\mathbb{Q})\}$  is the projection of  $\mathbb{Q}$  on  $\mathcal{C}$ . Note that, contrary to Lemma 6, (Csiszár, 1975, Theorem 2.2) is given for the *forward* Kullback–Leibler divergence whereas Lemma 6 is given for the *reverse* KL divergence. In addition, (Csiszár, 1975, Theorem 2.2) requires the projection set  $\mathcal{C}$  to be convex which is not satisfied for the space of Markov measures  $\mathcal{M}$ , see Appendix D. Using Lemma 6, we have the following proposition.

**Proposition 7.** *Under mild assumptions, we have  $\lim_{n \rightarrow +\infty} \text{KL}(\mathbb{P}^n|\mathbb{P}^{n+1}) = 0$ . If  $\mathbb{P}^*$  is a fixed point of  $(\mathbb{P}^n)_{n \in \mathbb{N}}$ , then  $\mathbb{P}^*$  is the Schrödinger Bridge  $\mathbb{P}^{\text{SB}}$ .*

Hence, the Markov path measures  $(\mathbb{P}^{2n+1})_{n \in \mathbb{N}}$  are getting closer to the reciprocal class, while the reciprocal path measures  $(\mathbb{P}^{2n+2})_{n \in \mathbb{N}}$  are getting closer to the set of Markov measures. Proposition 7 should be compared with (Rüschendorf, 1995, Proposition 2.1, Equation (2.16)) which shows that, for the IPF sequence  $(\mathbb{P}^n)_{n \in \mathbb{N}}$ , we have  $\lim_{n \rightarrow +\infty} \text{KL}(\mathbb{P}^{n+1}|\mathbb{P}^n) = 0$ . This is a result similar to Proposition 7 but for the *forward* Kullback–Leibler divergence. We leave the general study of the convergence of  $(\mathbb{P}^n)_{n \in \mathbb{N}}$  for future work.

## 4 Diffusion Schrödinger Bridge Matching

In this section, we present Diffusion Schrödinger Bridge Matching (DSBM), a practical algorithm for solving the SB problem obtained by combining the IMF procedure with Bridge Matching. Before presenting DSBM, we recall that the IMF sequence is given by  $(\mathbb{P}^n)_{n \in \mathbb{N}}$  in (8). We further denote  $\mathbb{M}^{n+1} = \mathbb{P}^{2n+1} \in \mathcal{M}$  and  $\Pi^n = \mathbb{P}^{2n} \in \mathcal{R}(\mathbb{Q})$ .

**Iterative Markovian Fitting in practice.** IMF alternatively projects on the set of Markov path measures  $\mathcal{M}$  and on the reciprocal class of  $\mathbb{Q}$ . Assuming we know how to sample from the bridge  $\mathbb{Q}_{|0,T}$  given the initial and terminal conditions, sampling from the reciprocal projection  $\text{proj}_{\mathcal{R}(\mathbb{Q})}(\mathbb{M})$  is simple and goes as follows. First, sample  $(\mathbf{X}_0, \mathbf{X}_T)$  from the joint distribution  $\mathbb{M}_{0,T}$ <sup>5</sup>. Then, sample from the bridge  $\mathbb{Q}_{|0,T}(\cdot|\mathbf{X}_0, \mathbf{X}_T)$ .

The bottleneck of IMF is in the computation of the Markovian projections  $\mathbb{M}^* = \text{proj}_{\mathcal{M}}(\Pi)$ . Using Definition 1, we get that  $\mathbb{M}^* = \text{proj}_{\mathcal{M}}(\Pi)$  is associated with the process

$$d\mathbf{X}_t = \{f_t(\mathbf{X}_t) + \sigma_t^2 \mathbb{E}_{\Pi_{T|t}}[\nabla \log \mathbb{Q}_{T|t}(\mathbf{X}_T|\mathbf{X}_t) | \mathbf{X}_t]\}dt + \sigma_t d\mathbf{B}_t, \quad \mathbf{X}_0 \sim \pi_0.$$

By Proposition 2, we can learn  $\mathbb{M}^*$  using  $\mathbb{M}^{\theta^*}$  given by

$$d\mathbf{X}_t = \{f_t(\mathbf{X}_t) + v_{\theta^*}(t, \mathbf{X}_t)\}dt + \sigma_t d\mathbf{B}_t, \quad \mathbf{X}_0 \sim \pi_0, \quad (9)$$

$$\theta^* = \text{argmin}_{\theta} \left\{ \int_0^T \mathbb{E}_{\Pi_{t,T}} [\|\sigma_t^2 \nabla \log \mathbb{Q}_{T|t}(\mathbf{X}_T|\mathbf{X}_t) - v_{\theta}(t, \mathbf{X}_t)\|^2] / \sigma_t^2 dt : \theta \in \Theta \right\}, \quad (10)$$

and  $\{v_{\theta} : \theta \in \Theta\}$  is a parametric family of functions, usually given by a neural network. Suppose the family of functions  $\{v_{\theta} : \theta \in \Theta\}$  is rich enough, we have for any  $t \in [0, T]$  and  $x_t \in \mathbb{R}^d$ , the optimal  $v_{\theta^*}(t, x_t) = \sigma_t^2 \mathbb{E}_{\Pi_{T|t}}[\nabla \log \mathbb{Q}_{T|t}(\mathbf{X}_T|\mathbf{X}_t) | \mathbf{X}_t = x_t]$ .

With the above two procedures for computing  $\text{proj}_{\mathcal{R}(\mathbb{Q})}(\mathbb{M})$  and  $\text{proj}_{\mathcal{M}}(\Pi)$ , we can now describe a numerical method implementing IMF. Let  $\Pi^0 = \int \mathbb{Q}_{|0,T} d\Pi_{0,T}^0$  be such that  $\Pi_0^0 = \pi_0$ ,  $\Pi_T^0 = \pi_T$ . Following (8), let  $\mathbb{M}^1 \approx \text{proj}_{\mathcal{M}}(\Pi^0)$  given by (9) with  $v_{\theta^*}$  learned using (10). Next, sample from  $\Pi^1 = \text{proj}_{\mathcal{R}(\mathbb{Q})}(\mathbb{M}^1)$  by sampling from  $\mathbb{M}_{0,T}^1$  and reconstructing the bridge  $\mathbb{Q}_{|0,T}$ . The Markov measure  $\mathbb{M}^2 \approx \text{proj}_{\mathcal{M}}(\Pi^1)$  is obtained similarly to  $\mathbb{M}^1$ . We iterate the process to obtain a sequence  $(\Pi^n, \mathbb{M}^{n+1})_{n \in \mathbb{N}}$ . In practice, this algorithm performs poorly, since due to the approximate minimization (10) to compute  $\mathbb{M}^{n+1}$ , we do not have  $\mathbb{M}_T^{n+1} = \pi_T$  as in Proposition 2. Instead, we incur a bias for each  $n \in \mathbb{N}$ , and this bias between  $\mathbb{M}_T^{n+1}$  and  $\pi_T$  accumulates.

To mitigate this problem, we alternate between a *forward* Markovian projection and a *backward* Markovian projection. This procedure is justified by the following proposition.

<sup>5</sup>In practice, we sample the SDE associated with  $\mathbb{M}$  and save a batch of joint samples  $(\mathbf{X}_0, \mathbf{X}_T)$ . This is similar to the *trajectory caching* procedure in De Bortoli et al. (2021), but we only retain initial and final samples.

**Proposition 8.** Assume that  $\Pi = \int \mathbb{Q}_{|0,T} d\Pi_{0,T}$  with  $\mathbb{Q}$  associated with  $d\mathbf{X}_t = f_t(\mathbf{X}_t)dt + \sigma_t d\mathbf{B}_t$ . Under mild conditions, the Markovian projection  $\mathbb{M}^* = \text{proj}_{\mathcal{M}}(\Pi)$  is associated with both

$$d\mathbf{X}_t = \{f_t(\mathbf{X}_t) + \sigma_t^2 \mathbb{E}_{\Pi_{T|t}}[\nabla \log \mathbb{Q}_{T|t}(\mathbf{X}_T | \mathbf{X}_t) | \mathbf{X}_t]\}dt + \sigma_t d\mathbf{B}_t, \quad \mathbf{X}_0 \sim \Pi_0, \quad (11)$$

$$d\mathbf{Y}_t = \{-f_{T-t}(\mathbf{Y}_t) + \sigma_{T-t}^2 \mathbb{E}_{\Pi_{0|T-t}}[\nabla \log \mathbb{Q}_{T-t|0}(\mathbf{Y}_t | \mathbf{Y}_T) | \mathbf{Y}_t]\}dt + \sigma_{T-t} d\mathbf{B}_t, \quad \mathbf{Y}_0 \sim \Pi_T. \quad (12)$$

In Proposition 8, (11) is the definition of the Markovian projection, see Definition 1. However, (12) is an equivalent representation as a *time-reversal*. In practice,  $(\mathbf{Y}_t)_{t \in [0,T]}$  is approximated with

$$d\mathbf{Y}_t = \{-f_{T-t}(\mathbf{Y}_t) + v_{\phi^*}(T-t, \mathbf{Y}_t)\}dt + \sigma_{T-t} d\mathbf{B}_t, \quad \mathbf{Y}_0 \sim \pi_T, \quad (13)$$

$$\phi^* = \text{argmin}_{\phi} \left\{ \int_0^T \mathbb{E}_{\Pi_{0,t}} [\|\sigma_t^2 \nabla \log \mathbb{Q}_{t|0}(\mathbf{X}_t | \mathbf{X}_0) - v_{\phi}(t, \mathbf{X}_t)\|^2] / \sigma_t^2 dt : \phi \in \Phi \right\}. \quad (14)$$

Suppose the family of functions  $\{v_{\phi} : \phi \in \Phi\}$  is rich enough, we have for any  $t \in [0, T]$  and  $x_t \in \mathbb{R}^d$ , the optimal  $v_{\phi^*}(t, x_t) = \sigma_t^2 \mathbb{E}_{\Pi_{0,t}}[\nabla \log \mathbb{Q}_{t|0}(\mathbf{X}_t | \mathbf{X}_0) | \mathbf{X}_t = x_t]$ .

Note that in the forward projection  $\mathbf{X}_0 \sim \pi_0$ , while in the backward projection  $\mathbf{Y}_0 \sim \pi_T$ . Therefore, using the backward projection removes the bias on  $\pi_T$  accumulated from the previous iterations. Alternating between (13) and (9) yields the Diffusion Schrödinger Bridge Matching (DSBM) methodology summarized in Algorithm 1.

---

**Algorithm 1** Diffusion Schrödinger Bridge Matching

---

- 1: **Input:** Joint distribution  $\Pi_{0,T}^0$ , tractable bridge  $\mathbb{Q}_{|0,T}$ , number of outer iterations  $N \in \mathbb{N}$ .
  - 2: Let  $\Pi^0 = \int \mathbb{Q}_{|0,T} d\Pi_{0,T}^0$ .
  - 3: **for**  $n \in \{0, \dots, N-1\}$  **do**
  - 4:   Learn  $v_{\phi^*}$  using (14) with  $\Pi = \Pi^{2n}$ .
  - 5:   Let  $\mathbb{M}^{2n+1}$  be given by (13).
  - 6:   Let  $\Pi^{2n+1} = \int \mathbb{Q}_{|0,T} d\mathbb{M}_{0,T}^{2n+1}$ .
  - 7:   Learn  $v_{\theta^*}$  using (10) with  $\Pi = \Pi^{2n+1}$ .
  - 8:   Let  $\mathbb{M}^{2n+2}$  be given by (9).
  - 9:   Let  $\Pi^{2n+2} = \int \mathbb{Q}_{|0,T} d\mathbb{M}_{0,T}^{2n+2}$ .
  - 10: **end for**
  - 11: **Output:**  $v_{\theta^*}, v_{\phi^*}$
- 

Algorithm 1 leverages the time-symmetry of the Markovian projection by alternating between the backward and forward Markovian projections. However, it is possible to learn *both* the forward and backward processes at each step. This also allows us to consider a *consistency* loss which enforces that the backward and forward processes match, see Appendix G.

In the next paragraph, we relate Algorithm 1 to the DSB algorithm (De Bortoli et al., 2021) which relies on the classical IPF.

**Initialization coupling.** If instead of initializing DSBM by a coupling between  $\pi_0, \pi_T$ , we initialize it by  $\Pi_{0,T}^0 = \mathbb{Q}_{0,T}$  where  $\mathbb{Q}_0 = \pi_0$  and  $\mathbb{Q}_T \neq \pi_T$ <sup>6</sup> is given by the reference process defined in (1), then DSBM recovers the IPF iterates used in DSB. In particular, we have the following identification.

**Proposition 9.** Suppose the families of functions  $\{v_{\theta} : \theta \in \Theta\}$  and  $\{v_{\phi} : \phi \in \Phi\}$  are rich enough so that they can model the optimal vector fields. Let  $(\Pi^n, \mathbb{M}^{n+1})_{n \in \mathbb{N}}$  be the optimal DSBM sequence in Algorithm 1 initialized with  $\Pi_{0,T}^0 = \mathbb{Q}_{0,T}$ , and let  $(\tilde{\Pi}^n)_{n \in \mathbb{N}}$  be the optimal DSB sequence given by the IPF iterates in (7). Then for any  $n \in \mathbb{N}, n \geq 1$ , we have  $\mathbb{M}^n = \tilde{\Pi}^n$ .

The training procedure in DSBM is very different from the one in DSB (De Bortoli et al., 2021; Chen et al., 2022). In existing works, for any  $n \in \mathbb{N}$ ,  $\tilde{\Pi}^{2n+1}$  is obtained as the time-reversal of  $\tilde{\Pi}^{2n}$ , see (De Bortoli et al., 2021, Proposition 6). More precisely, for any  $n \in \mathbb{N}$  we have that  $\tilde{\Pi}^{2n+1}$  is associated with  $d\mathbf{Y}_t^{2n+1} = b_{T-t}^n(\mathbf{Y}_t^{2n+1})dt + d\mathbf{B}_t$ ,  $\mathbf{Y}_0 \sim \pi_T$  and  $\tilde{\Pi}^{2n+2}$  with  $d\mathbf{X}_t^{2n+2} = f_t^{n+1}(\mathbf{X}_t^{2n+2})dt + d\mathbf{B}_t$ ,  $\mathbf{X}_0 \sim \pi_0$ , where  $b_t^n = -f_t^n + \nabla \log \tilde{\Pi}_t^{2n}$  and  $f_t^{n+1} = -b_t^n + \nabla \log \tilde{\Pi}_t^{2n+1}$ . The drifts  $b_t^n$  and  $f_t^n$  are estimated using the *drift-matching loss*. This requires sampling time-discretized trajectories from  $\tilde{\Pi}^{2n}$  in order to estimate  $b_t^n$ . In contrast, in Algorithm 1 we do not use the full trajectory of  $\mathbb{M}^{2n}$  to learn  $\mathbb{M}^{2n+1}$ . More precisely, we only use the *coupling*  $\mathbb{M}_{0,T}^{2n}$  to create the bridge measure  $\Pi^{2n} = \int \mathbb{Q}_{|0,T} d\mathbb{M}_{0,T}^{2n}$ . By doing so, (i) the losses (10) and (14) can be evaluated for any time  $t \in [0, T]$ , without relying on a fixed *time-discretization* of the process; (ii) setting  $\Pi^{2n} = \int \mathbb{Q}_{|0,T} d\mathbb{M}_{0,T}^{2n}$  projects  $\mathbb{M}^{2n}$  on the reciprocal class of  $\mathbb{Q}$ , see Definition 3. While every

---

<sup>6</sup>If  $\mathbb{Q}_T$  were equal to  $\pi_T$ , then the SB would be given by  $\mathbb{Q}$ .

iteration  $\tilde{\mathbb{P}}^n$  in the DSB algorithm is supposed to be in the reciprocal class of  $\mathbb{Q}$ , in practice one can observe a *forgetting* of the bridge  $\mathbb{Q}_{|0,T}$  (Fernandes et al., 2021). In DSBM, this effect is countered by considering explicit projections on the reciprocal class; (iii) the *trajectory caching* procedure in DSBM is more computationally and memory efficient, since the Bridge Matching objective does not require evaluating the drift at two different timesteps as in DSB (thus only requiring half NFEs), nor saving the entire SDE trajectory in memory. We explain further the benefits of DSBM in Appendix F.

We call DSBM-IPF, the DSBM algorithm applied with the coupling given by the forward reference process  $\Pi_{0,T}^0 = \mathbb{Q}_{0,T}$ . Similarly, we call DSBM-IMF, the DSBM algorithm applied with an initial independent coupling  $\Pi_{0,T}^0 = \pi_0 \otimes \pi_T$ . We experiment with both methods and leave extensive empirical comparison between the two as future work.

**On DSBM and existing algorithms.** Different choices of bridges  $\mathbb{Q}_{|0,T}$  and couplings  $\Pi_{0,T}^0$  in Algorithm 1 recover existing algorithms. For the independent coupling  $\Pi_{0,T}^0 = \pi_0 \otimes \pi_T$  and Brownian bridge  $\mathbb{Q}_{|0,T}$  with diffusion parameter  $\sigma_t = \sigma$  given by (3), we get that (10) recovers the Brownian Bridge Matching loss (4). Letting  $\sigma \rightarrow 0$ , we recover Flow Matching (Lipman et al., 2023). In this case, further iterations repeating lines 7-9 in Algorithm 1 recover the Rectified Flow algorithm (Liu et al., 2023b). Therefore, existing Flow Matching and Rectified Flow approaches can be seen as special limiting cases of DSBM with only forward projections. If the coupling  $\Pi_{0,T}^0$  is given by an estimation of the OT map, then the first iteration recovers the OT-CFM model (Tong et al., 2023). Finally for general bridges  $\mathbb{Q}_{|0,T}$ , if instead we are given the optimal Schrödinger Bridge static coupling  $\Pi_{0,T}^0 = \Pi_{0,T}^{\text{SB}}$ , then the DSBM procedure converges in one iteration and we recover Somnath et al. (2023). See Section 5 for further discussions.

**Probability flow ODE.** At equilibrium of DSBM, we have that  $(\mathbf{Y}_t)_{t \in [0,T]}$  given by (13) is the time reversal of  $(\mathbf{X}_t)_{t \in [0,T]}$  given by (9) and are both associated with the Schrödinger Bridge path measure. As a result, we have that  $v_{\phi^*}(t, x) = -v_{\theta^*}(t, x) + \sigma_t^2 \nabla \log \mathbb{P}_t^{\text{SB}}(x)$ . Hence, a probability flow  $(\mathbf{Z}_t)_{t \in [0,T]}$  such that  $\text{Law}(\mathbf{Z}_t) = \mathbb{P}_t^{\text{SB}}$  for any  $t \in [0, T]$  is given by

$$d\mathbf{Z}_t = \{f_t(\mathbf{Z}_t) + \frac{1}{2}[v_{\theta^*}(t, \mathbf{Z}_t) - v_{\phi^*}(t, \mathbf{Z}_t)]\}dt, \quad \mathbf{Z}_0 \sim \pi_0.$$

Note that the path measure induced by  $(\mathbf{Z}_t)_{t \in [0,T]}$  does not correspond to  $\mathbb{P}^{\text{SB}}$ ; in particular,  $(\mathbf{Z}_0, \mathbf{Z}_T)$  is *not* an entropic optimal transport plan. However, since for any  $t \in [0, T]$ ,  $\mathbf{Z}_t$  has marginal distribution  $\mathbb{P}_t^{\text{SB}}$ , we can compute the log-likelihood of the model (Song et al., 2021b; Huang et al., 2021).

## 5 Related Work

**Markovian projection and Bridge Matching.** The concept of Markovian projection has been rediscovered multiple times. It was first introduced in the probability literature by Gyöngy (1986) to mimic non-Markovian processes, following on a work by Krylov (1984). This idea was introduced in mathematical finance community by Dupire (1994). In the machine learning context, this was first proposed by Peluchetti (2021) to define Bridge Matching models. More recently, Liu et al. (2022b) established Kullback–Leibler divergence properties of the Markovian projection presented in Proposition 2, the first part of Lemma 6, and applied Bridge Matching for learning data on discrete and constrained domains.

**Bridge and Flow Matching.** Flow Matching Models correspond to deterministic bridges with deterministic samplers (ODEs) and have been under active study (Liu et al., 2023b; Liu, 2022; Lipman et al., 2023; Albergo and Vanden-Eijnden, 2023; Tong et al., 2023; Heitz et al., 2023). Denoising Diffusion Implicit Models (DDIM) (Song et al., 2021a) can also be thought of as a discrete-time version of Flow Matching, see Liu et al. (2023b). These models were extended to the Riemannian setting by Chen and Lipman (2023). Recently, Albergo et al. (2023) studied the influence of stochasticity in the sampler and the bridge, through the concept of stochastic interpolants<sup>7</sup>. Liu et al. (2023a); Delbracio and Milanfar (2023) used Bridge Matching to perform image restoration tasks and

<sup>7</sup>Stochastic interpolants do not require the reference measure  $\mathbb{Q}$  to be Markov. We discuss the differences between our frameworks in Appendix B.



noted benefits of stochasticity empirically. Closely related to our work is the Rectified Flow algorithm of Liu et al. (2023b), which corresponds to an iterative Flow Matching procedure in order to improve the straightness of the flow and thus ease its simulation. DSBM-IMF is closest to Rectified Flow, which can be seen as the deterministic limiting case as  $\sigma \rightarrow 0$ . However, there are a few important differences. Firstly, we adopt the SDE approach as opposed to the ODE approach in Rectified Flow. This distinction is crucial in theory, as Proposition 5, which guarantees the uniqueness of the characterization of SB, is valid only when  $\sigma_t > 0$ . Consequently, Rectified Flow is not guaranteed to converge to the dynamic optimal transport solution. In a following work Liu (2022) established formal connections between Rectified Flow and OT when restricting the class of vector fields to gradient fields. In DSBM, the connection to OT is obtained by considering its entropy-regularized version. Secondly, Rectified Flow also performs Markovian projections iteratively, but only in the forward direction. Consequently, the bias in the marginal  $\mathbb{P}_T^p$  is accumulated and cannot be corrected in later iterations, i.e. the first iteration will achieve the most accurate marginal  $\mathbb{P}_T^1$ . Subsequent iterations can improve the straightness of the flow and thus requires few discretization steps, but at the cost of the optimal sampling accuracy. We observe in practice that this becomes particularly problematic if the first iteration of Rectified Flow fails to provide a good transport. In our methodology, we leverage Proposition 8 to perform forward and backward Bridge Matching, and we observe that the marginal accuracy is able to improve with each iteration.

**Diffusion Schrödinger Bridge.** Schrödinger Bridges (Schrödinger, 1932) are ubiquitous in probability theory (Léonard, 2014b) and stochastic control (Dai Pra, 1991; Chen et al., 2021). More recently, they have been used in machine learning to solve generative modeling problems. In particular, De Bortoli et al. (2021) proposed the DSB algorithm, and Vargas et al. (2021); Chen et al. (2022) proposed similar related algorithms. The case where one of the terminal distributions is a Dirac delta mass is investigated in Wang et al. (2021). These methods were later extended to solve conditional simulation problems (Shi et al., 2022) and more general control problems (Thornton et al., 2022; Liu et al., 2022a; Chen et al., 2023; Tamir et al., 2023). In Somnath et al. (2023), Schrödinger Bridges are trained using one Bridge Matching iteration, assuming access to the Schrödinger static coupling. Our proposed method DSBM-IPF most closely resembles DSB, but with improved continuous-time training and projections on the reciprocal class which mitigate two limitations of DSB.

## 6 Experiments

### 6.1 2D Experiments

We first show our proposed methods can learn lower kinetic energy transport maps and generate correct samples in some 2D examples. We compare our method DSBM with DSB (De Bortoli et al., 2021), Flow Matching (FM) (Lipman et al., 2023), Conditional Flow Matching (CFM), OT-CFM (Tong et al., 2023), and Rectified Flow (RF) (Liu et al., 2023b). OT-CFM directly uses sample-based Optimal Transport solver (Flamary et al., 2021) to approximate the solution of the dynamic OT problem, whereas the rest of the methods do not use OT solvers. DSB and our proposed method learn the EOT map implicitly as the solution of the diffusion process. Note that FM cannot be used for the *moons-8gaussians* task since it requires a Gaussian source, but CFM is applicable. For our method, we use Brownian motion for the reference measure  $\mathbb{Q}$  with Brownian bridge (3) and  $\sigma_t = 1$  in all cases, except the *moons-8gaussians* dataset where we use  $\sigma_t = 5$ .

In Table 2, we show the 2-Wasserstein distance between the test set and the generated samples when using 20 discretization steps, as well as the average path energy using each method. The path energy is defined by  $\mathbb{E}[\int_0^T \|v(t, \mathbf{Z}_t)\|^2 dt]$  where  $v$  is the learned drift along the ODE trajectory  $\mathbf{Z}_t$ . Lower path energies represent shorter (and potentially easier to integrate) trajectories. For the 2D experiments, we observe that OT-CFM performs the best by directly utilizing OT solvers. On the other hand, DSBM and Rectified Flow achieve lower 2-Wasserstein distance and path energy among methods that do not use specialized solvers. Comparing DSBM and Rectified Flow, we observe that Rectified Flow achieves lower sampling error under 20 steps except for the *moons-8gaussians* dataset, for which DSBM is significantly more accurate. Since RF can be seen as the deterministic limit case of DSBM, this suggests that the optimal amount of stochasticity may depend on the task. Compared to FM and CFM, DSBM provides consistent improvements over both sampling quality and path energy. Furthermore, while DSBM solves the same SB problems as DSB, DSBM outperforms DSB

Table 2: Sampling quality as measured by 2-Wasserstein distance and path energy for the 2D experiments.  $\pm$  one standard deviation computed over 5 seeds. Best values are in bold and second best are italicized.

	(a)				(b)			
	<i>2-Wasserstein (Euler 20 steps)</i>				<i>Path energy</i>			
	moons	scurve	8gaussians	moons-8gaussians	moons	scurve	8gaussians	moons-8gaussians
DSBM-IPF	0.140±0.006	0.140±0.024	0.315±0.079	<i>0.812±0.092</i>	1.598±0.034	2.110±0.059	<i>14.91±0.310</i>	42.16±1.026
DSBM-IMF	0.144±0.024	0.145±0.037	0.338±0.091	0.838±0.098	1.580±0.036	2.092±0.053	<b>14.81±0.255</b>	41.00±1.495
DSB	0.190±0.049	0.272±0.065	0.411±0.084	0.987±0.324	-	-	-	-
FM	0.212±0.025	0.161±0.033	0.351±0.066	-	2.227±0.056	2.950±0.074	18.12±0.416	-
CFM	0.215±0.028	0.171±0.023	0.370±0.049	1.285±0.314	2.391±0.043	3.071±0.026	18.00±0.090	116.5±2.633
RF	<i>0.129±0.022</i>	<i>0.126±0.019</i>	<i>0.267±0.041</i>	1.522±0.304	<i>1.185±0.052</i>	<i>1.633±0.074</i>	<i>14.84±0.441</i>	<i>37.61±3.906</i>
OT-CFM	<b>0.111±0.005</b>	<b>0.102±0.013</b>	<b>0.253±0.040</b>	<b>0.716±0.187</b>	<b>1.178±0.020</b>	<b>1.577±0.036</b>	15.10±0.215	<b>30.50±0.626</b>

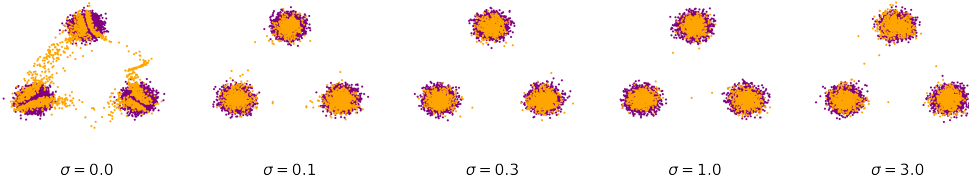


Figure 2: Samples from final marginal of learned SB process (yellow) versus ground truth (purple).

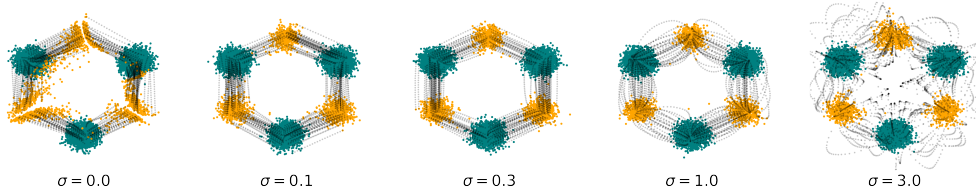


Figure 3: Trajectories of ODE integration of the learned SB probability flow.

in terms of 2-Wasserstein distance on all datasets at the same sampling budget, which suggests that DSBM solves the SB problem with higher accuracy.

### 6.1.1 Variance of the reference measure $\mathbb{Q}$

We now investigate the effect of the value of  $\sigma_t$  used for the reference path measure  $\mathbb{Q}$ . We assume a time-homogeneous  $\sigma_t = \sigma$  value for simplicity. In Figures 2 and 3, we vary  $\sigma$  and visualize the learned transport for the *3gaussians* problem of transporting between two Gaussian mixtures. In Table 3 we show the 2-Wasserstein distance between the test set and generated samples for this *3gaussians* problem as well as the *moons-8gaussians* problem. We find that large values of  $\sigma$  result in increasingly curved transport paths, and correspondingly reduced performance when  $\sigma$  is excessively large. Conversely, we also find reduced performance when  $\sigma$  is excessively small. This is due to increased optimization difficulty and bias accumulation. Firstly, the number of outer steps required to converge to the Schrödinger Bridge is proportional to the KL divergence between the reference process and the Schrödinger Bridge itself. This KL divergence increases as  $\sigma$  is taken to 0 thus making the outer optimization convergence more difficult. Further, the introduction of a small amount of noise also decreases optimization difficulty by smoothing the intermediate marginals between the two terminal distributions. Finally, a larger  $\sigma$  value can also increase the diversity of sampled couplings and may alleviate some bias accumulation issues during outer iterations. When  $\sigma = 0$ , these issues result in the artifacts observed in Figure 2. The appropriate value for  $\sigma$  depends on the spatial scaling of the problem as shown in Table 3 where the optimum  $\sigma$  is larger for the larger scale *moons-8gaussians* problem. The benefit of setting  $\sigma > 0$  and using a stochastic sampler was also observed in Albergo et al. (2023); Delbracio and Milanfar (2023).

Table 3: 2-Wasserstein distance for varying value of  $\sigma$  used in the DSBM-IMF method.

3gaussians		moons-8gaussians	
$\sigma$	2-Wasserstein	$\sigma$	2-Wasserstein
$\sigma = 0$	0.646±0.028	$\sigma = 0$	1.459±0.008
$\sigma = 0.1$	0.724±0.039	$\sigma = 1.0$	1.285±0.346
$\sigma = 0.3$	0.546±0.169	$\sigma = 2.0$	0.916±0.292
$\sigma = 1.0$	<b>0.439±0.072</b>	$\sigma = 4.0$	<b>0.818±0.249</b>
$\sigma = 3.0$	0.543±0.078	$\sigma = 8.0$	0.989±0.179

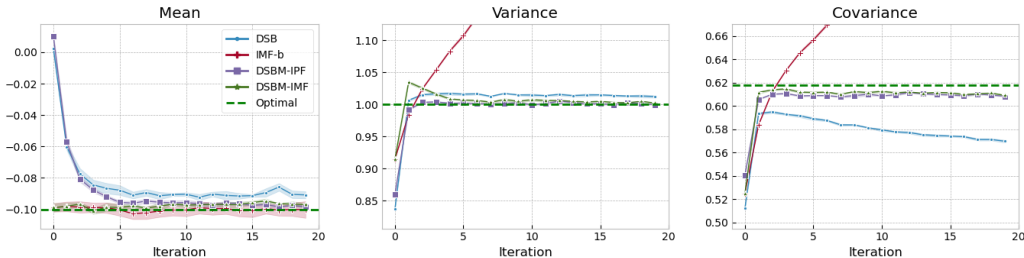


Figure 4: Convergence of Gaussian experiment in dimension  $d = 50$ .  $\pm$  one standard deviation computed over 5 seeds is shaded.

## 6.2 High-Dimensional Synthetic Experiment

We next perform the Gaussian transport experiment in De Bortoli et al. (2021) with dimension  $d = 50$  to verify the scalability of our proposed approach. The true SB can be computed analytically in this case (De Bortoli et al., 2021; Bunne et al., 2023). In Figure 4, we plot the convergence of DSB and our proposed methods. We also consider a baseline IMF-b, which performs Iterative Markovian Fitting numerically but only in the backward direction. All methods converge approximately to the mean of ground truth distribution  $\pi_0$ . However, the variance estimate becomes increasingly inaccurate for IMF-b as the number of iterations increases. On the other hand, our proposed methods do not suffer from this issue, which demonstrates the usefulness of alternating forward and backward training. Furthermore, for the covariance between times 0, 1 under the true SB  $\mathbb{P}^{\text{SB}}$ , our proposed methods converge close to the ground truth covariance, whereas DSB and IMF-b both worsen from the optimum. In particular, DSB loses accuracy due to accumulation of error in its iterative time-reversal procedure as noted in De Bortoli et al. (2021). Our proposed methods are the most accurate across all three metrics and avoided the deterioration of learned bridges.

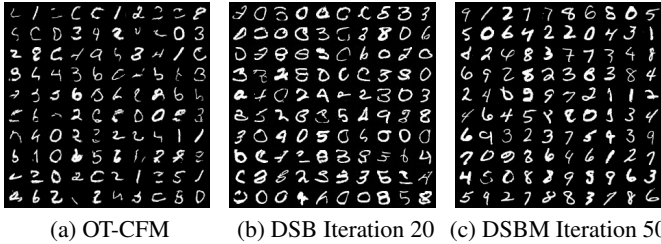
In Table 4, we further quantify the accuracy of the learned SB by computing the KL divergence between the marginal distributions of the learned processes  $\mathbb{P}_t$  and the true SB marginal  $\mathbb{P}_t^{\text{SB}}$ . We also compare with SB-CFM (Tong et al., 2023) using this setup at the marginal level. Our proposed methods achieve similar KL divergence as SB-CFM in dimension  $d = 5$ , but are much more accurate in higher dimensions compared to both DSB and SB-CFM. This highlights the challenge of learning SB in high dimensions. On the other hand, the error of DSBM scales approximately linearly with the number of dimensions, which suggests that our proposed method is more scalable.

## 6.3 Image Experiment

Finally, we test our method on image domain transfer between MNIST digits and EMNIST letters as in De Bortoli et al. (2021). We compare our method DSBM-IPF as a direct substitute of DSB, and also with CFM, OT-CFM and Rectified Flow. Similar to De Bortoli et al. (2021), we use the set of first 5 letters of EMNIST in upper and lower cases (A-E, a-e) such that both domains have 10 classes in total. Both DSB and DSBM integrate the learned SDE with 30 Euler-Maruyama integration steps, whereas we use 100 Euler steps for all flow methods.

Table 4: Average  $\text{KL}(\mathbb{P}_t^{\text{P}}|\mathbb{P}_t^{\text{SB}})$  at 21 uniformly spaced values of  $t \in [0, T]$  for the Gaussian experiment in dimensions  $d = 5, 20, 50$ .  $\pm$  one standard deviation computed over 5 seeds. Best values are in bold and second best are italicized.

$\text{KL} \times 10^{-3}$	$d = 5$	$d = 20$	$d = 50$
DSB	3.26 $\pm$ 1.60	13.0 $\pm$ 3.49	32.8 $\pm$ 1.28
SB-CFM	1.45 $\pm$ 0.73	12.3 $\pm$ 1.47	49.4 $\pm$ 3.91
DSBM-IPF	<b>1.23<math>\pm</math>0.23</b>	<b>4.42<math>\pm</math>0.76</b>	<b>8.75<math>\pm</math>0.87</b>
DSBM-IMF	<i>1.34<math>\pm</math>0.51</i>	<i>5.05<math>\pm</math>0.95</i>	<i>9.76<math>\pm</math>1.67</i>



(a) OT-CFM (b) DSB Iteration 20 (c) DSBM Iteration 50

Figure 5: Samples of MNIST digits transferred from letters.

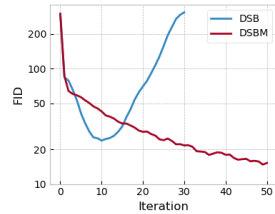


Figure 6: FID vs iteration.

We plot some output samples from each algorithm in Figure 5 and the convergence of FID score in Figure 6, and additional experimental results are included in Appendix I.3. We find that in this high-dimensional transfer example, OT-CFM produces samples of worse quality (Figure 5a). This suggests that OT-CFM becomes less and less applicable in higher dimensions. Since Rectified Flow cannot improve training errors in CFM, its performance is also worse than CFM and OT-CFM on this task (Figure 7b). On the other hand, DSB appears to generate clearer samples after 20 iterations as shown in Figure 5b. However, DSB’s FID score deteriorates after 10 iterations, and eventually becomes exceedingly high after 30 iterations. Our method DSBM achieves higher quality samples visually, and does not suffer from deterioration. We train DSBM for 50 outer iterations, and do not observe deterioration of FID score. Our method is also about 30% more efficient than DSB in terms of runtime due to computational savings discussed in Section 4 and Appendix F.

## 7 Discussion

In this work, we propose IMF, a novel methodology for learning Schrödinger Bridges motivated by recent progress in Flow Matching (Liu et al., 2023b; Lipman et al., 2023). IMF is an alternative to the classical IPF and can be interpreted as its dual, with alternative projections on the class of Markov and reciprocal processes. Building on IPF and the novel IMF methodologies, we present two practical algorithms, DSBM-IPF and DSBM-IMF, to compute SBs. The DSBM framework mitigates the time-discretization and accumulation of bias issues in existing methods such as DSB (De Bortoli et al., 2021) as demonstrated in our experiments. In future work, we would like to further investigate the theoretical properties of DSBM. Another interesting direction would be to compare DSBM-IMF vs DSBM-IPF, and investigate whether one could propose better initial couplings scalable to high dimensions to further accelerate the convergence of DSBM. We believe IMF might also be useful to develop a better understanding of the Rectified Flow procedure (Liu et al., 2023b), as IMF minimizes a clear objective and Rectified Flow is informally a limiting case of it. Finally, the Rectified Flow procedure has been extended to solve OT problems with general convex costs by Liu (2022), and it would be interesting to derive a SB version of this approach.

## References

- Albergo, M. S., Boffi, N. M., and Vanden-Eijnden, E. (2023). Stochastic interpolants: A unifying framework for flows and diffusions. *arXiv preprint arXiv:2303.08797*.
- Albergo, M. S. and Vanden-Eijnden, E. (2023). Building normalizing flows with stochastic interpolants. In *International Conference on Learning Representations*.
- Anderson, B. D. (1982). Reverse-time diffusion equation models. *Stochastic Processes and their Applications*, 12(3):313–326.
- Banerjee, A., Guo, X., and Wang, H. (2005). On the optimality of conditional expectation as a Bregman predictor. *IEEE Transactions on Information Theory*, 51(7):2664–2669.
- Benamou, J.-D. and Brenier, Y. (2000). A computational fluid mechanics solution to the Monge–Kantorovich mass transfer problem. *Numerische Mathematik*, 84(3):375–393.
- Benamou, J.-D., Carlier, G., Cuturi, M., Nenna, L., and Peyré, G. (2015). Iterative Bregman projections for regularized transportation problems. *SIAM Journal on Scientific Computing*, 37(2):A1111–A1138.
- Bernton, E., Heng, J., Doucet, A., and Jacob, P. E. (2019). Schrödinger bridge samplers. *arXiv preprint arXiv:1912.13170*.
- Bogachev, V. I., Krasovitskii, T. I., and Shaposhnikov, S. V. (2021). On uniqueness of probability solutions of the Fokker-Planck-Kolmogorov equation. *Sbornik: Mathematics*, 212(6):745.
- Bunne, C., Hsieh, Y.-P., Cuturi, M., and Krause, A. (2023). The Schrödinger bridge between Gaussian measures has a closed form. In *International Conference on Artificial Intelligence and Statistics*.
- Bunne, C., Papaxanthos, L., Krause, A., and Cuturi, M. (2022). Proximal optimal transport modeling of population dynamics. In *International Conference on Artificial Intelligence and Statistics*, pages 6511–6528. PMLR.
- Caluya, K. F. and Halder, A. (2021). Wasserstein proximal algorithms for the Schrödinger bridge problem: Density control with nonlinear drift. *IEEE Transactions on Automatic Control*, 67(3):1163–1178.
- Caron, M., Misra, I., Mairal, J., Goyal, P., Bojanowski, P., and Joulin, A. (2020). Unsupervised learning of visual features by contrasting cluster assignments. In *Advances in Neural Information Processing Systems*.
- Chen, R. T. and Lipman, Y. (2023). Riemannian flow matching on general geometries. *arXiv preprint arXiv:2302.03660*.
- Chen, T., Liu, G.-H., Tao, M., and Theodorou, E. A. (2023). Deep momentum multi-marginal Schrödinger bridge. *arXiv preprint arXiv:2303.01751*.
- Chen, T., Liu, G.-H., and Theodorou, E. A. (2022). Likelihood training of Schrödinger bridge using forward-backward SDEs theory. In *International Conference on Learning Representations*.
- Chen, Y., Georgiou, T., and Pavon, M. (2016). Entropic and displacement interpolation: a computational approach using the Hilbert metric. *SIAM Journal on Applied Mathematics*, 76(6):2375–2396.
- Chen, Y., Georgiou, T. T., and Pavon, M. (2021). Optimal transport in systems and control. *Annual Review of Control, Robotics, and Autonomous Systems*, 4.
- Chung, K. L. and Walsh, J. B. (2006). *Markov processes, Brownian motion, and Time Symmetry*, volume 249. Springer Science & Business Media.
- Courty, N., Flamary, R., Habrard, A., and Rakotomamonjy, A. (2017). Joint distribution optimal transportation for domain adaptation. In *Advances in Neural Information Processing Systems*.
- Csiszár, I. (1975). I-divergence geometry of probability distributions and minimization problems. *The Annals of Probability*, 3(1):146–158.

- Cuturi, M. (2013). Sinkhorn distances: Lightspeed computation of optimal transport. In *Advances in Neural Information Processing Systems*.
- Dai Pra, P. (1991). A stochastic control approach to reciprocal diffusion processes. *Applied Mathematics and Optimization*, 23(1):313–329.
- De Bortoli, V., Thornton, J., Heng, J., and Doucet, A. (2021). Diffusion Schrödinger bridge with applications to score-based generative modeling. In *Advances in Neural Information Processing Systems*.
- Delbraccio, M. and Milanfar, P. (2023). Inversion by direct iteration: An alternative to denoising diffusion for image restoration. *arXiv preprint arXiv:2303.11435*.
- Dupire, B. (1994). Pricing with a smile. *Risk*, 7(1):18–20.
- Essid, M. and Pavon, M. (2019). Traversing the Schrödinger bridge strait: Robert Fortet’s marvelous proof redux. *Journal of Optimization Theory and Applications*, 181(1):23–60.
- Fernandes, D. L., Vargas, F., Ek, C. H., and Campbell, N. D. (2021). Shooting Schrödinger’s cat. In *Fourth Symposium on Advances in Approximate Bayesian Inference*.
- Feydy, J., Charlier, B., Vialard, F.-X., and Peyré, G. (2017). Optimal transport for diffeomorphic registration. In *Medical Image Computing and Computer Assisted Intervention- MICCAI*, pages 291–299.
- Finlay, C., Gerolin, A., Oberman, A. M., and Pooladian, A.-A. (2020). Learning normalizing flows from entropy-Kantorovich potentials. *arXiv preprint arXiv:2006.06033*.
- Flamary, R., Courty, N., Gramfort, A., Alaya, M. Z., Boisbunon, A., Chambon, S., Chapel, L., Corenflos, A., Fatras, K., Fournier, N., Gautheron, L., Gayraud, N. T., Janati, H., Rakotomamonjy, A., Redko, I., Rolet, A., Schutz, A., Seguy, V., Sutherland, D. J., Tavenard, R., Tong, A., and Vayer, T. (2021). Pot: Python optimal transport. *Journal of Machine Learning Research*, 22(78):1–8.
- Föllmer, H. (1988). Random fields and diffusion processes. In *École d’Été de Probabilités de Saint-Flour XV–XVII, 1985–87*, pages 101–203. Springer.
- Fortet, R. (1940). Résolution d’un système d’équations de M. Schrödinger. *Journal de Mathématiques Pures et Appliquées*, 1:83–105.
- Goodfellow, I. J., Pouget-Abadie, J., Mirza, M., Xu, B., Warde-Farley, D., Ozair, S., Courville, A., and Bengio, Y. (2014). Generative adversarial networks. *arXiv preprint arXiv:1406.2661*.
- Gyöngy, I. (1986). Mimicking the one-dimensional marginal distributions of processes having an ito differential. *Probability Theory and Related Fields*, 71:501–516.
- Hausmann, U. G. and Pardoux, E. (1986). Time reversal of diffusions. *The Annals of Probability*, 14(4):1188–1205.
- Heitz, E., Belcour, L., and Chambon, T. (2023). Iterative  $\alpha$ -(de)blending: Learning a deterministic mapping between arbitrary densities. <https://openreview.net/forum?id=s7gnrEtWSm>.
- Ho, J., Jain, A., and Abbeel, P. (2020). Denoising diffusion probabilistic models. In *Advances in Neural Information Processing Systems*.
- Huang, C.-W., Lim, J. H., and Courville, A. C. (2021). A variational perspective on diffusion-based generative models and score matching. In *Advances in Neural Information Processing Systems*.
- Hyvärinen, A. (2005). Estimation of non-normalized statistical models by score matching. *Journal of Machine Learning Research*, 6(4).
- Krylov, N. (1984). Once more about the connection between elliptic operators and Itô’s stochastic equations. In *Statistics and Control of Stochastic Processes, Steklov Seminar*, pages 214–229.
- Kullback, S. (1968). Probability densities with given marginals. *The Annals of Mathematical Statistics*, 39(4):1236–1243.

- Léonard, C. (2012). Girsanov theory under a finite entropy condition. In *Séminaire de Probabilités XLIV*, pages 429–465. Springer.
- Léonard, C. (2014a). Some properties of path measures. In *Séminaire de Probabilités XLVI*, pages 207–230. Springer.
- Léonard, C. (2014b). A survey of the Schrödinger problem and some of its connections with optimal transport. *Discrete & Continuous Dynamical Systems-A*, 34(4):1533–1574.
- Léonard, C., Røelly, S., Zambrini, J.-C., et al. (2014). Reciprocal processes. a measure-theoretical point of view. *Probability Surveys*, 11:237–269.
- Lipman, Y., Chen, R. T., Ben-Hamu, H., Nickel, M., and Le, M. (2023). Flow matching for generative modeling. In *International Conference on Learning Representations*.
- Liu, G.-H., Chen, T., So, O., and Theodorou, E. A. (2022a). Deep generalized Schrödinger bridge. *arXiv preprint arXiv:2209.09893*.
- Liu, G.-H., Vahdat, A., Huang, D.-A., Theodorou, E. A., Nie, W., and Anandkumar, A. (2023a). I<sup>2</sup>SB: Image-to-image Schrödinger bridge. *arXiv preprint arXiv:2302.05872*.
- Liu, Q. (2022). Rectified flow: A marginal preserving approach to optimal transport. *arXiv preprint arXiv:2209.14577*.
- Liu, X., Gong, C., and Liu, Q. (2023b). Flow straight and fast: Learning to generate and transfer data with rectified flow. In *International Conference on Learning Representations*.
- Liu, X., Wu, L., Ye, M., and Liu, Q. (2022b). Let us build bridges: Understanding and extending diffusion generative models. *arXiv preprint arXiv:2208.14699*.
- Mikami, T. and Thieullen, M. (2008). Optimal transportation problem by stochastic optimal control. *SIAM Journal on Control and Optimization*, 47(3):1127–1139.
- Palmowski, Z. and Rolski, T. (2002). A technique for exponential change of measure for Markov processes. *Bernoulli*, pages 767–785.
- Pavon, M., Trigila, G., and Tabak, E. G. (2021). The data-driven Schrödinger bridge. *Communications on Pure and Applied Mathematics*, 74:1545–1573.
- Peluchetti, S. (2021). Non-denoising forward-time diffusions. <https://openreview.net/forum?id=oVfIKuhqfC>.
- Peyré, G. and Cuturi, M. (2019). Computational optimal transport. *Foundations and Trends® in Machine Learning*, 11(5-6):355–607.
- Rogers, L. C. G. and Williams, D. (2000). *Diffusions, Markov processes, and Martingales. Vol. 2*. Cambridge Mathematical Library. Cambridge University Press, Cambridge. Itô calculus, Reprint of the second (1994) edition.
- Rüschendorf, L. (1995). Convergence of the iterative proportional fitting procedure. *The Annals of Statistics*, 23(4):1160–1174.
- Rüschendorf, L. and Thomsen, W. (1993). Note on the Schrödinger equation and  $i$ -projections. *Statistics & Probability letters*, 17(5):369–375.
- Schrödinger, E. (1932). Sur la théorie relativiste de l'électron et l'interprétation de la mécanique quantique. *Annales de l'Institut Henri Poincaré*, 2(4):269–310.
- Shi, Y., De Bortoli, V., Deligiannidis, G., and Doucet, A. (2022). Conditional simulation using diffusion Schrödinger bridges. In *Uncertainty in Artificial Intelligence*.
- Sinkhorn, R. (1967). Diagonal equivalence to matrices with prescribed row and column sums. *The American Mathematical Monthly*, 74(4):402–405.
- Somnath, V. R., Pariset, M., Hsieh, Y.-P., Martinez, M. R., Krause, A., and Bunne, C. (2023). Aligned diffusion Schrödinger bridges. *arXiv preprint arXiv:2302.11419*.

- Song, J., Meng, C., and Ermon, S. (2021a). Denoising diffusion implicit models. In *International Conference on Learning Representations*.
- Song, K.-U. (2022). Applying regularized Schrödinger-bridge-based stochastic process in generative modeling. *arXiv preprint arXiv:2208.07131*.
- Song, Y., Sohl-Dickstein, J., Kingma, D. P., Kumar, A., Ermon, S., and Poole, B. (2021b). Score-based generative modeling through stochastic differential equations. In *International Conference on Learning Representations*.
- Tamir, E., Trapp, M., and Solin, A. (2023). Transport with support: Data-conditional diffusion bridges. *arXiv preprint arXiv:2301.13636*.
- Thornton, J., Hutchinson, M., Mathieu, E., De Bortoli, V., Teh, Y. W., and Doucet, A. (2022). Riemannian diffusion Schrödinger bridge. *arXiv preprint arXiv:2207.03024*.
- Tong, A., Malkin, N., Huguet, G., Zhang, Y., Rector-Brooks, J., Fatras, K., Wolf, G., and Bengio, Y. (2023). Conditional flow matching: Simulation-free dynamic optimal transport. *arXiv preprint arXiv:2302.00482*.
- Vargas, F., Thodoroff, P., Lamacraft, A., and Lawrence, N. (2021). Solving Schrödinger bridges via maximum likelihood. *Entropy*, 23(9):1134.
- Villani, C. (2009). *Optimal transport*, volume 338 of *Grundlehren der Mathematischen Wissenschaften [Fundamental Principles of Mathematical Sciences]*. Springer-Verlag, Berlin. Old and new.
- Vincent, P. (2011). A connection between score matching and denoising autoencoders. *Neural Computation*, 23(7):1661–1674.
- Wang, G., Jiao, Y., Xu, Q., Wang, Y., and Yang, C. (2021). Deep generative learning via Schrödinger bridge. In *International Conference on Machine Learning*.



## Outline of the Appendix

In Appendix A, we first clarify the relationship between different Flow Matching Models in the existing literature and show that Bridge Matching generalizes Flow Matching. In Appendix B, we draw a link between the parameterization of bridges in this paper and the stochastic interpolant in Albergo et al. (2023). In Appendix C, we give proofs for results in the main text. In Appendix D, we give a simple counter-example proving that the set of Markov measures is not convex. In Appendix E, we derive a discrete-time version of Markovian projection. In Appendix F, we explain further the benefits of DSBM compared to DSB. In Appendix G, we describe a method for learning the forward and backward processes jointly and propose a consistency loss between the forward and backward processes. In Appendix H, we present a practical scaling of the loss function to reduce the variance, similar to standard Denoising Diffusion Models. In Appendix I, we give further details for all experiments and some additional experimental results.

## A Bridge Matching and Flow Matching Models

In this section, we clarify the relationship between variants of Bridge Matching and Flow Matching and show that they are equivalent under some conditions. We follow the nomenclature of Tong et al. (2023). We refer to the algorithm originally proposed in Lipman et al. (2023) using linear probability paths and described in (Tong et al., 2023, Section 4.1) as Flow Matching (FM), and the algorithm proposed in (Tong et al., 2023, Section 4.2) as Conditional Flow Matching (CFM). There is a small constant parameter  $\sigma_{\min}$  in both algorithms, which controls the smoothing of the modeled distribution. We consider the case  $\sigma_{\min} = 0$ . Then we show that CFM recovers exactly the 1st iteration of Rectified Flow (Liu et al., 2023b). Furthermore, FM, CFM and the 1st iteration of Rectified Flow are all equivalent when performing generative modeling with a standard Gaussian  $\pi_0$ . We refer to them collectively as Flow Matching Models (FMMs) as they only differ in the smoothing method. We also present them all under the Bridge Matching framework. These models can also be interpreted in the context of *stochastic interpolants* (Albergo and Vanden-Eijnden, 2023; Albergo et al., 2023). Finally, we present recent applications of Bridge Matching and show that some of the objectives in Somnath et al. (2023); Liu et al. (2023a); Delbracio and Milanfar (2023) are identical.

**Flow Matching and Conditional Flow Matching.** In Flow Matching (FM), the objective (Lipman et al., 2023, Equation (21)) is

$$\mathbb{E}_{\Pi_{t,T}} [\|(\mathbf{X}_T - \mathbf{X}_t)/(T - t) - v_\theta(t, \mathbf{X}_t)\|^2],$$

where  $\Pi_{t,T}$  is given by  $\pi_T(\mathbf{X}_T)N(\mathbf{X}_t; \frac{t}{T}\mathbf{X}_T, (1 - \frac{t}{T})^2)$ .

In Conditional Flow Matching (CFM),  $\mathbf{X}_t^{0,T} = \frac{t}{T}\mathbf{X}_T + (1 - \frac{t}{T})\mathbf{X}_0$ , with  $\mathbf{X}_0 \sim N(0, \text{Id})$  and the objective (Tong et al., 2023, Equation (16)) is given by

$$\mathbb{E}_{\Pi_{0,T}} [\|(\mathbf{X}_T - \mathbf{X}_0)/T - v_\theta(t, \mathbf{X}_t^{0,T})\|^2]. \quad (15)$$

This is the same as (Liu et al., 2023b, Equation (1)). Furthermore,  $(\mathbf{X}_T - \mathbf{X}_0)/T = (1 - \frac{t}{T})(\mathbf{X}_T - \mathbf{X}_0)/(T - t) = (\mathbf{X}_T - \mathbf{X}_t^{0,T})/(T - t)$ , so the CFM objective is equivalent to

$$\mathbb{E}_{\Pi_{t,T}} [\|(\mathbf{X}_T - \mathbf{X}_t^{0,T})/(T - t) - v_\theta(t, \mathbf{X}_t^{0,T})\|^2]. \quad (16)$$

In the case of generative modeling,  $\pi_0$  is a standard Gaussian distribution and  $\Pi_{0,T}$  is given by  $N(\mathbf{X}_0; 0, \text{Id})\pi_T(\mathbf{X}_T)$ . Thus,  $\Pi_{t,T}$  is also given by  $\pi_T(\mathbf{X}_T)N(\mathbf{X}_t^{0,T}; \frac{t}{T}\mathbf{X}_T, (1 - \frac{t}{T})^2)$ . Therefore, the FM (Lipman et al., 2023) and CFM (Tong et al., 2023) objectives are exactly the same. However, CFM is also applicable when  $\pi_0$  is not Gaussian distributed, so CFM is a generalized version of FM<sup>8</sup>.

**Stochastic Interpolant.** In (Albergo and Vanden-Eijnden, 2023; Albergo et al., 2023), the concept of stochastic interpolant is introduced. In Albergo and Vanden-Eijnden (2023), the interpolation is deterministic (not necessarily linear), of the form  $I_t(x_0, x_T) = \alpha(t)x_0 + \beta(t)x_T$ , while in Albergo

<sup>8</sup>In the case  $\sigma_{\min} > 0$ , FM and CFM are indeed different in how smoothing is performed, and we refer to Tong et al. (2023) for a more detailed analysis.

et al. (2023), the interpolation is stochastic given by  $I_t(x_0, x_T, z) = \alpha(t)x_0 + \beta(t)x_T + \gamma(t)\mathbf{Z}$  for  $\mathbf{Z} \sim \mathcal{N}(0, \text{Id})$ . In Albergo and Vanden-Eijnden (2023), an ODE is learned and the associated velocity field  $v_\theta$  is obtained by minimizing the following objective (Albergo and Vanden-Eijnden, 2023, Equation (9))

$$\mathbb{E}_{\Pi_0, T} [\|\partial_t I_t(\mathbf{X}_0, \mathbf{X}_T) - v_\theta(t, \mathbf{X}_t^{0, T})\|^2].$$

Hence, if  $I_t(x_0, x_T) = \frac{t}{T}x_0 + (1 - \frac{t}{T})x_T$ , we recover (15).

**Link with Bridge Matching.** When  $\sigma \rightarrow 0$  in Bridge Matching, we recover the same objective (4) as the CFM objective (16), since  $\nabla \log \mathbb{Q}_{T|t}(\mathbf{X}_T | \mathbf{X}_t) = (\mathbf{X}_T - \mathbf{X}_t)/(\sigma^2(T-t))$ . Bridge Matching can also be applied to general distributions  $\pi_0, \pi_T$ ; i.e.  $\pi_0$  does not have to be restricted to a Gaussian. Therefore, Bridge Matching is a generalized version of CFM, see also (Liu et al., 2022b, Equation (10)).

**Inverse problems and interpolation.** Somnath et al. (2023) present a bridge matching algorithm to interpolate between aligned data  $(\mathbf{X}_0, \mathbf{X}_T) \sim \Pi_{0, T}$ . The objective in (Somnath et al., 2023, Equation (8)) is identical (setting  $g_t = 1$ ) to the FM objective or the Bridge Matching objective (3). In the case  $g_t = 1$ , the measure  $\mathbb{Q}_{|0, T}$  is associated with  $d\mathbf{X}_t^{0, T} = (x_T - \mathbf{X}_t^{0, T})/(T-t)dt + d\mathbf{B}_t$ , which is identical to the second part of (3). Setting  $\sigma_t = 1$ , we recover the same objective in Liu et al. (2023a). The measure  $\mathbb{Q}_{|0, T}$  is given by (Liu et al., 2023a, Proposition 3.3) which, in the case  $g_t = 1$ , is identical to the second part of (3). The main difference between Liu et al. (2023a) and Somnath et al. (2023) resides in the choice of  $\Pi_{0, T}$ . In the case of Somnath et al. (2023), this choice is motivated by the access to *aligned data* with applications to biology assuming they are distributed as the true Schrödinger static coupling, i.e.  $\Pi_{0, T} = \Pi_{0, T}^{\text{SB}}$ , whereas in Liu et al. (2023a),  $\Pi_{0, T}$  corresponds to a pairing between clean and corrupted images.

Finally, in (Delbracio and Milanfar, 2023, Equation (5)) the authors consider a reconstruction process of the form

$$d\mathbf{X}_t = (\mathbb{E}_{\Pi_{0|t}}[\mathbf{X}_0 | \mathbf{X}_t] - \mathbf{X}_t)/tdt, \quad \mathbf{X}_T \sim \Pi_T, \quad (17)$$

where here we have replaced  $F(x_t, t)$  by  $\mathbb{E}_{\Pi_{0|t}}[\mathbf{X}_0 | \mathbf{X}_t = x_t]$ . This is justified if the  $\|\cdot\|_p$  norm in (Delbracio and Milanfar, 2023, Equation (4)) is replaced by  $\|\cdot\|_2^2$  (or any Bregman Loss Function, see Banerjee et al. (2005)). In Delbracio and Milanfar (2023),  $\Pi_{0, T}$  corresponds to the joint distribution of clean and corrupted images as in Liu et al. (2023a).  $\Pi_0 = \pi_0$  is the distribution of clean images and  $\Pi_T = \pi_T$  is the distribution of corrupted images. Exchanging the role of  $\Pi_0$  and  $\Pi_T$ , (17) can be rewritten as

$$d\mathbf{X}_t = (\mathbb{E}_{\Pi_{T|t}}[\mathbf{X}_T | \mathbf{X}_t] - \mathbf{X}_t)/(T-t)dt, \quad \mathbf{X}_0 \sim \Pi_0.$$

Equivalently, we obtain the optimal CFM vector field in (16). Note that Delbracio and Milanfar (2023) also incorporates a stochastic version of their objective (Delbracio and Milanfar, 2023, Equation (7)). It remains an open question whether this objective can be understood as a special instance of the bridge matching framework.

## B The Design Space of Brownian Bridges

**From stochastic interpolants to Brownian bridges.** In this section, we draw a link between our parameterization of bridges and the one used in Albergo et al. (2023). In Albergo et al. (2023), a stochastic interpolant is defined as

$$\mathbf{X}_t = \bar{\alpha}_t x_0 + \bar{\beta}_t x_T + \bar{\gamma}_t \mathbf{Z}, \quad (18)$$

where  $\mathbf{Z} \sim \mathcal{N}(0, \text{Id})$ . Since their methodology and analysis mainly relies on the probability flow, they work with (18), which is easier to analyse. In our setting, as we deal mostly with diffusions, it is natural to parameterize Brownian bridges as follows

$$d\mathbf{X}_t = \{-\alpha_t \mathbf{X}_t + \beta_t x_T\}dt + \gamma_t d\mathbf{B}_t. \quad (19)$$

The goal of this section is to derive explicit formulas between the parameters  $\bar{\alpha}_t, \bar{\beta}_t$  and  $\bar{\gamma}_t$  of (18) and the parameters  $\alpha_t, \beta_t$  and  $\gamma_t$  of (19). Consider  $(\mathbf{X}_t)_{t \in [0, T]}$  given by (19). We have that for any  $t \in [0, T]$

$$\mathbf{X}_t = \exp[-A_t]x_0 + \int_0^t \beta_s \exp[A_s - A_t]ds x_T + \int_0^t \gamma_s \exp[A_s - A_t]d\mathbf{B}_s,$$

where  $A_t = \int_0^t \alpha_s ds$ . Therefore, we have that

$$\bar{\alpha}_t = \exp[-\int_0^t \alpha_s ds], \quad \bar{\beta}_t = \int_0^t \beta_s \exp[-\int_s^t \alpha_u du] ds, \quad \bar{\gamma}_t^2 = \int_0^t \gamma_s^2 \exp[-2\int_s^t \alpha_u du] ds, \quad (20)$$

$$\alpha_t = -\frac{\bar{\alpha}'_t}{\bar{\alpha}_t}, \quad \beta_t = \bar{\beta}'_t + \bar{\beta}_t \alpha_t, \quad \gamma_t^2 = (\bar{\gamma}_t^2)' + 2\bar{\gamma}_t^2 \alpha_t = 2\bar{\gamma}_t \bar{\gamma}'_t + 2\bar{\gamma}_t^2 \alpha_t. \quad (21)$$

Using this relationship, we get that the Markovian projection, see Definition 1, is given by

$$d\mathbf{X}_t^* = f_t^*(\mathbf{X}_t) dt + \gamma_t d\mathbf{B}_t, \quad f_t^*(x_t) = \mathbb{E}_{\Pi_{T|t}}[-\alpha_t \mathbf{X}_t + \beta_t x_T \mid \mathbf{X}_t = x_t].$$

We have that

$$\begin{aligned} f_t^*(x_t) &= \mathbb{E}_{\Pi_{T|t}}[-\alpha_t \mathbf{X}_t + \beta_t x_T \mid \mathbf{X}_t = x_t] \\ &= \mathbb{E}_{\Pi_{0,T|t}}[-\alpha_t(\bar{\alpha}_t x_0 + \bar{\beta}_t x_T + \bar{\gamma}_t \mathbf{Z}) + \beta_t x_T \mid \mathbf{X}_t = x_t]. \end{aligned}$$

Using (21), we get that

$$f_t^*(x_t) = \mathbb{E}_{\Pi_{0,T|t}}[\bar{\alpha}'_t x_0 + \bar{\beta}'_t x_T + \frac{\bar{\alpha}'_t \bar{\gamma}_t}{\bar{\alpha}_t} \mathbf{Z} \mid \mathbf{X}_t = x_t].$$

In Albergo et al. (2023), it is shown that  $\nabla \log \mathbb{M}_t^*(x_t) = -\mathbb{E}_{\Pi_{0,T|t}}[\mathbf{Z} \mid \mathbf{X}_t = x_t]/\bar{\gamma}_t$ , where  $\mathbb{M}^*$  is the Markovian projection. The probability flow associated with  $(\mathbf{X}_t^*)_{t \in [0,T]}$  is given by

$$\begin{aligned} d\mathbf{Z}_t^* &= \{f_t^*(\mathbf{Z}_t^*) - \frac{\gamma_t^2}{2} \nabla \log p_t(\mathbf{Z}_t^*)\} dt \\ &= \{\mathbb{E}_{\Pi_{0,T|t}}[\bar{\alpha}'_t x_0 + \bar{\beta}'_t x_T + (-\alpha_t \bar{\gamma}_t + \frac{\gamma_t^2}{2\bar{\gamma}_t}) \mathbf{Z} \mid \mathbf{X}_t = \mathbf{Z}_t^*]\} dt \\ &= \{\mathbb{E}_{\Pi_{0,T|t}}[\bar{\alpha}'_t x_0 + \bar{\beta}'_t x_T + \bar{\gamma}'_t \mathbf{Z} \mid \mathbf{X}_t = \mathbf{Z}_t^*]\} dt. \end{aligned}$$

Hence, we recover (Albergo et al., 2023, Theorem 2.6).

**Non-Markov path measures.** A natural question is whether (19) arises as the bridge measure of some Markov measure. For instance, if  $\mathbb{Q}$  is associated with  $(x_0 + \mathbf{B}_t)_{t \in [0,T]}$ , then pinning the process at  $x_T$  at time  $T$ , we get that the associated bridge measure  $\mathbb{Q}_{|0,T}$  is given by

$$d\mathbf{X}_t^{0,T} = (x_T - \mathbf{X}_t)/(T-t) dt + d\mathbf{B}_t.$$

Therefore, we recover (19) with  $\alpha_t = \beta_t = \frac{1}{T-t}$  and  $\gamma_t = 1$ . Using (20), we get that  $\bar{\alpha}_t = 1 - \frac{t}{T}$ ,  $\bar{\beta}_t = \frac{t}{T}$  and  $\bar{\gamma}_t^2 = (T-t)t/T$ . We recover (3), upon noting that  $\mathbf{B}_t - \frac{t}{T}\mathbf{B}_T$  is Gaussian with zero mean and variance  $(T-t)t/T$ .

More generally, we consider a Markov measure  $\mathbb{Q}$  associated with  $(\mathbf{X}_t)_{t \in [0,T]}$  such that

$$d\mathbf{X}_t = -a_t \mathbf{X}_t dt + c_t d\mathbf{B}_t, \quad \mathbf{X}_0 = x_0.$$

We now derive the associated bridge measure  $\mathbb{Q}_{|0,T}$ :

$$\mathbf{X}_T = \exp[-\Lambda_T + \Lambda_t] \mathbf{X}_t + \int_t^T c_s \exp[\Lambda_s - \Lambda_T] d\mathbf{B}_s,$$

with  $\Lambda_t = \int_0^t a_s ds$ . We have that

$$\begin{aligned} c_t^2 \nabla_{x_t} \log \mathbb{Q}_{T|t}(x_T | x_t) &= (c_t^2 \exp[\Lambda_t - \Lambda_T] / \int_t^T c_s^2 \exp[2(\Lambda_s - \Lambda_T)] ds) x_T \\ &\quad - (c_t^2 \exp[2(\Lambda_t - \Lambda_T)] / \int_t^T c_s^2 \exp[2(\Lambda_s - \Lambda_T)] ds) x_t. \end{aligned}$$

Therefore, combining this result and (2), we get that  $\mathbb{Q}_{|0,T}$  is associated with

$$\begin{aligned} \alpha_t &= a_t + c_t^2 \exp[-2\int_t^T a_s ds] / \int_t^T c_s^2 \exp[-2\int_s^T a_u du] ds, \\ \beta_t &= c_t^2 \exp[-\int_t^T a_s ds] / \int_t^T c_s^2 \exp[-2\int_s^T a_u du] ds, \quad \gamma_t = c_t. \end{aligned}$$

In that case  $(a_t, c_t)_{t \in [0,T]}$  entirely parameterize  $(\alpha_t, \beta_t, \gamma_t)_{t \in [0,T]}$ . Hence, in the Ornstein-Uhlenbeck setting, if  $\mathbb{Q}_{|0,T}$  is the bridge of a Markov measure, it is fully parameterized by two functions while in the non-Markov setting it is parameterized by three functions.

In this paper, we present our framework in the Markovian setting as the Schrödinger Bridge problem is usually defined with respect to Markov reference measures. However, our methodology could be extended in a straightforward fashion to the non-Markovian setting. This would allow for a further exploration of the design space of DSBM.

## C Proofs

### C.1 Proof of Proposition 2

We refer the reader to [Chung and Walsh \(2006\)](#); [Rogers and Williams \(2000\)](#) for an introduction to Doob  $h$ -transform. Our theoretical treatment of the Doob  $h$ -transform closely follows [Palmowski and Rolski \(2002\)](#).

First, we introduce the *infinitesimal generator*  $\mathcal{A}$  given for any  $f \in C_c^\infty([0, T] \times \mathbb{R}^d, \mathbb{R})$ ,  $t \in [0, T]$  and  $x \in \mathbb{R}^d$  by

$$\mathcal{A}f(t, x) = \langle f_t(x), \nabla f(t, x) \rangle + \frac{\sigma_t^2}{2} \Delta f(t, x) + \partial_t f(t, x). \quad (22)$$

The following assumption ensures that the diffusion associated with  $\mathbb{Q}$  as well as its Markovian projections are well-defined.

**A1.**  $f$ ,  $\sigma$  and  $(t, x_t) \mapsto \mathbb{E}_{\Pi_{T|t}}[\nabla \log \mathbb{Q}_{T|t}(\mathbf{X}_T | \mathbf{X}_t) | \mathbf{X}_t = x_t]$  are locally Lipschitz and there exist  $C > 0$ ,  $\psi \in C([0, T], \mathbb{R}_+)$  such that for any  $t \in [0, T]$  and  $x_0, x_t \in \mathbb{R}^d$ , we have

$$\begin{aligned} \|f_t(x_t)\| &\leq C(1 + \|x_t\|), & C &\geq \sigma_t \geq 1/C, \\ \|\mathbb{E}_{\Pi_{T|t}}[\nabla \log \mathbb{Q}_{T|t}(\mathbf{X}_T | \mathbf{X}_t) | \mathbf{X}_t = x_t]\| &\leq C\psi(t)(1 + \|x_t\|). \end{aligned}$$

We consider the following assumption, which will ensure that we can apply Doob  $h$ -transform techniques.

**A2.** For any  $x_0 \in \mathbb{R}^d$ ,  $\Pi_{T|0}$  is absolutely continuous w.r.t.  $\mathbb{Q}_{T|0}$ . For any  $x_0 \in \mathbb{R}^d$ , let  $\varphi_{T|0}$  be given for any  $x_T \in \mathbb{R}^d$  by  $\varphi_{T|0}(x_T | x_0) = d\Pi_{T|0}(x_T | x_0) / d\mathbb{Q}_{T|0}(x_T | x_0)$  and assume that for any  $x_0 \in \mathbb{R}^d$ ,  $x_T \mapsto \varphi_{T|0}(x_T | x_0)$  is bounded. For any  $x_0 \in \mathbb{R}^d$ , let  $\varphi_{t|0}$  given for any  $x_t \in \mathbb{R}^d$  and  $t \in [0, T]$  by

$$\varphi_{t|0}(x_t | x_0) = \int_{\mathbb{R}^d} \varphi_{T|0}(x_T | x_0) d\mathbb{Q}_{T|t}(x_T | x_t). \quad (23)$$

Finally, we assume that for any  $x_0 \in \mathbb{R}^d$ ,  $(t, x_t) \mapsto 1/\varphi_{t|0}(x_t | x_0)$  and  $(t, x_t) \mapsto \mathcal{A}\varphi_{t|0}(x_t | x_0)$  are bounded.

This means that for any  $x_0 \in \mathbb{R}^d$ ,  $(t, x_t) \mapsto \varphi_t(x_t | x_0)$  is a *good function* in the sense of ([Palmowski and Rolski, 2002](#), Proposition 3.2). Note here that these assumptions could be relaxed on a case-by-case basis. We leave this study for future work.

The following lemma, is a direct consequence of **A2** and (23). It ensures that the  $h$ -function  $\varphi_{t|0}$  satisfies the backward Kolmogorov equation.

**Lemma 10.** Assume **A2**. Then,  $\varphi \in C^{1,2}([0, T] \times \mathbb{R}^d, \mathbb{R})$  and  $\mathcal{A}\varphi_0 = 0$ .

Using (22), we have that for any  $x_0 \in \mathbb{R}^d$  and  $f \in C_c^\infty([0, T] \times \mathbb{R}^d, \mathbb{R})$ ,  $t \in [0, T]$  and  $x_t \in \mathbb{R}^d$

$$(\mathcal{A}(f\varphi_0) - f\mathcal{A}\varphi_0)(t, x_t) / \varphi_0(t, x_t) = \mathcal{A}f(t, x_t) + \sigma_t^2 \langle \nabla f(t, x_t), \nabla \log \varphi_{t|0}(x_t | x_0) \rangle.$$

Finally, we consider the following assumption, which will ensure that the Doob  $h$ -transform is well-defined.

**A3.** For any  $x_0 \in \mathbb{R}^d$ , there exists  $C \geq 0$  such that for any  $t \in [0, T]$  and  $x_t \in \mathbb{R}^d$ ,  $\|\nabla \log \varphi_{t|0}(x_t | x_0)\| \leq C(1 + \|x_0\| + \|x_t\|)$ .

We are now ready to state and prove Proposition 2. Note that the Markovian projection is defined in Definition 1. Finally, we define  $\mathcal{M}$  the space of path measures such that  $\mathbb{P} \in \mathcal{M}$  if  $\mathbb{P}$  is associated with  $d\mathbf{X}_t = \{f_t(\mathbf{X}_t) + v_t(\mathbf{X}_t)\}dt + \sigma_t d\mathbf{B}_t$ , with  $\sigma, v$  locally Lipschitz. This restriction of Markov measures allows us to apply the entropic version of the Girsanov theorem ([Léonard, 2012](#)). It has no impact on our methodology.

**Proposition 11.** Assume **A1**, **A2**, **A3**. Let  $\mathbb{M}^* = \text{proj}_{\mathcal{M}}(\Pi)$ . Then,

$$\begin{aligned} \mathbb{M}^* &= \text{argmin}_{\mathbb{M}} \{\text{KL}(\Pi | \mathbb{M}) : \mathbb{M} \in \mathcal{M}\}, \\ \text{KL}(\Pi | \mathbb{M}^*) &= \frac{1}{2} \int_0^T \mathbb{E}_{\Pi_{0,t}} [\|\sigma_t^2 \mathbb{E}_{\Pi_{T|0,t}}[\nabla \log \mathbb{Q}_{T|t}(\mathbf{X}_T | \mathbf{X}_t) | \mathbf{X}_0, \mathbf{X}_t] - v_t^*\|^2] / \sigma_t^2 dt. \end{aligned}$$

In addition, we have that for any  $t \in [0, T]$ ,  $\mathbb{M}_t^* = \Pi_t$ . In particular,  $\mathbb{M}_T^* = \Pi_T$ .

*Proof.* First, we recall that  $\Pi$  is given by  $\Pi = \mathbb{Q}\varphi_{0,T}$  with  $\varphi_{0,T} = \frac{d\Pi_{0,T}}{d\mathbb{Q}_{0,T}}$ . In particular, we have  $\Pi|_0 = \mathbb{Q}|_0\varphi_{T|0}$ , where  $\varphi_{T|0} = \frac{d\Pi_{T|0}}{d\mathbb{Q}_{T|0}}$ . Therefore, using Lemma 10, (Palmowski and Rolski, 2002, Lemma 3.1, Lemma 4.1), the remark following (Palmowski and Rolski, 2002, Lemma 4.1), A1, A2 and A3, we get that  $\Pi|_0$  is Markov and associated with the distribution of  $(\mathbf{X}_t)_{t \in [0,T]}$  given for any  $t \in [0, T]$  by

$$\mathbf{X}_t = \int_0^t \{f_s(\mathbf{X}_s) + \sigma_s^2 \nabla \log \varphi_{s|0}(\mathbf{X}_s | \mathbf{X}_0)\} ds + \int_0^t \sigma_s d\mathbf{B}_s, \quad (24)$$

where for any  $t \in [0, T]$ ,  $x_0, x_t \in \mathbb{R}^d$  we recall that

$$\varphi_{t|0}(x_t | x_0) = \int_{\mathbb{R}^d} \varphi_{T|0}(x_T | x_0) d\mathbb{Q}_{T|t}(x_T | x_t). \quad (25)$$

First, we have that for any  $t \in [0, T]$ ,  $x_t, x_0 \in \mathbb{R}^d$

$$\mathbb{Q}_{t|0}(x_t | x_0) \varphi_{t|0}(x_t | x_0) = \int_{\mathbb{R}^d} \mathbb{Q}_{t|0,T}(x_t | x_T, x_0) d\Pi_{T|0}(x_T | x_0) = \Pi_{t|0}(x_t | x_0).$$

Therefore, we get that for any  $t \in [0, T]$  and  $x_t, x_0 \in \mathbb{R}^d$

$$\varphi_{t|0}(x_t | x_0) = \frac{d\Pi_{t|0}(x_t | x_0)}{d\mathbb{Q}_{t|0}(x_t | x_0)}. \quad (26)$$

In addition, we have the following identity for any  $t \in [0, T]$ ,  $x_0, x_t, x_T \in \mathbb{R}^d$

$$\mathbb{Q}_{T|0}(x_T | x_0) \mathbb{Q}_{t|0,T}(x_t | x_0, x_T) = \mathbb{Q}_{t|0}(x_t | x_0) \mathbb{Q}_{T|t}(x_T | x_t).$$

Using (25), this result and (26), we get that for any  $t \in [0, T]$  and  $x_0, x_t \in \mathbb{R}^d$

$$\begin{aligned} \nabla \log \varphi_{t|0}(x_t | x_0) &= \int_{\mathbb{R}^d} \frac{\Pi_{T|0}(x_T | x_0) \mathbb{Q}_{T|t}(x_T | x_t)}{\mathbb{Q}_{T|0}(x_T | x_0) \varphi_{t|0}(x_t | x_0)} \nabla \log \mathbb{Q}_{T|t}(x_T | x_t) dx_T \\ &= \int_{\mathbb{R}^d} \frac{\Pi_{T|0}(x_T | x_0) \mathbb{Q}_{t|0,T}(x_t | x_0, x_T)}{\mathbb{Q}_{t|0}(x_t | x_0) \varphi_{t|0}(x_t | x_0)} \nabla \log \mathbb{Q}_{T|t}(x_T | x_t) dx_T \\ &= \int_{\mathbb{R}^d} \frac{\Pi_{t,T|0}(x_t, x_T | x_0)}{\Pi_{t|0}(x_t | x_0)} \nabla \log \mathbb{Q}_{T|t}(x_T | x_t) dx_T \\ &= \int_{\mathbb{R}^d} \nabla \log \mathbb{Q}_{T|t}(x_T | x_t) d\Pi_{T|t,0}(x_T | x_t, x_0). \end{aligned}$$

Hence, combining this result and (24), we get

$$\mathbf{X}_t = \int_0^t \{f_s(\mathbf{X}_s) + \sigma_s^2 \mathbb{E}_{\Pi_{T|t,0}}[\nabla \log \mathbb{Q}_{T|t}(\mathbf{X}_T | \mathbf{X}_t) | \mathbf{X}_t, \mathbf{X}_0]\} ds + \int_0^t \sigma_s d\mathbf{B}_s.$$

Let  $\mathbb{M}$  be Markov defined by  $d\mathbf{X}_t = \{f_t(\mathbf{X}_t) + v_t(\mathbf{X}_t)\} dt + \sigma_t d\mathbf{B}_t$ , such that  $\text{KL}(\Pi | \mathbb{M}) < +\infty$  with  $\sigma, v$  locally Lipschitz. Using (Léonard, 2012, Theorem 2.3), we get that

$$\text{KL}(\Pi | \mathbb{M}) = \frac{1}{2} \int_0^T \mathbb{E}_{\Pi_{0,t}} [\|\sigma_t^2 \mathbb{E}_{\Pi_{T|t,0}}[\nabla \log \mathbb{Q}_{T|t}(\mathbf{X}_T | \mathbf{X}_t) | \mathbf{X}_t, \mathbf{X}_0] - v_t(\mathbf{X}_t)\|^2] / \sigma_t^2 dt.$$

In addition, we have that for any  $t \in [0, T]$ ,

$$\begin{aligned} &\mathbb{E}_{\Pi_{0,t}} [\|\sigma_t^2 \mathbb{E}_{\Pi_{T|t,0}}[\nabla \log \mathbb{Q}_{T|t}(\mathbf{X}_T | \mathbf{X}_t) | \mathbf{X}_t, \mathbf{X}_0] - v_t(\mathbf{X}_t)\|^2] \\ &\geq \mathbb{E}_{\Pi_{0,t}} [\|\sigma_t^2 \mathbb{E}_{\Pi_{T|t,0}}[\nabla \log \mathbb{Q}_{T|t}(\mathbf{X}_T | \mathbf{X}_t) | \mathbf{X}_t, \mathbf{X}_0] - v_t^*(\mathbf{X}_t)\|^2], \end{aligned}$$

where  $v_t^*(x_t) = \sigma_t^2 \mathbb{E}_{\Pi_{T|t}}[\nabla \log \mathbb{Q}_{T|t}(\mathbf{X}_T | \mathbf{X}_t) | \mathbf{X}_t = x_t]$  which concludes the first part of the proof. For the second part of the proof, we show that for any  $t \in [0, T]$ , we have  $\mathbb{M}_t^* = \Pi_t$ . First, we have that  $\mathbb{M}_t^*$  and  $\Pi_t$  satisfy the same Fokker-Planck equation, see (Peluchetti, 2021, Theorem 2) for instance. We conclude by uniqueness of the solutions of the Fokker-Planck equation under A1 and A3, see Bogachev et al. (2021) for instance.  $\square$

## C.2 Proof of Proposition 4

*Proof.* By the additive property of KL divergence (Léonard, 2014a),  $\text{KL}(\mathbb{P} | \Pi) = \text{KL}(\mathbb{P}_{0,T} | \Pi_{0,T}) + \mathbb{E}_{\mathbb{P}_{0,T}}[\text{KL}(\mathbb{P}_{|0,T} | \Pi_{|0,T})]$ . Restricting  $\Pi_{|0,T} = \mathbb{Q}_{|0,T}$  directly gives that the KL minimizer is  $\Pi^*$  with  $\Pi_{0,T}^* = \mathbb{P}_{0,T}$ , and thus  $\Pi^* = \int \mathbb{Q}_{|0,T} d\mathbb{P}_{0,T}$ .  $\square$

### C.3 Proof of Proposition 5

This result is a direct consequence of (Léonard, 2014b, Theorem 2.12), which we recall here for completeness.

**Proposition 12.** *Assume that  $\mathbb{Q} \in \mathcal{M}$ , that  $\mathbb{Q}_0 = \mathbb{Q}_T = \bar{\mathbb{Q}}$ , that for any  $x_0, x_T \in \mathbb{R}^d$ ,  $d\mathbb{Q}_{0,T}/d(\bar{\mathbb{Q}} \otimes \bar{\mathbb{Q}})(x_0, x_T) \geq \exp[-A(x_0) - A(x_T)]$  with  $A \geq 0$  measurable,  $\int_{\mathbb{R}^d \times \mathbb{R}^d} \exp[-B(x_0) - B(x_T)] d\mathbb{Q}(x_0, x_T) < +\infty$  with  $B \geq 0$  measurable. Assume that there exists  $t_0 \in (0, T)$  and  $\mathbb{X}$  measurable such that  $\mathbb{Q}_{t_0}(\mathbb{X}) > 0$  and for all  $x \in \mathbb{X}$ ,  $\mathbb{Q}_{0,T} \ll \mathbb{Q}_{0,T|t_0}(\cdot | \mathbf{X}_{t_0} = x)$ . In addition, assume that  $\text{KL}(\pi_0 | \bar{\mathbb{Q}}) < +\infty$ ,  $\text{KL}(\pi_T | \bar{\mathbb{Q}}) < +\infty$ ,  $\int_{\mathbb{R}^d} (A + B)(x_0) d\pi_0(x_0) < +\infty$ ,  $\int_{\mathbb{R}^d} (A + B)(x_T) d\pi_T(x_T) < +\infty$ .*

*Then there exists a unique Schrödinger Bridge  $\mathbb{P}^{\text{SB}}$ . In addition let  $\mathbb{P}$  be a Markov measure in the reciprocal class of  $\mathbb{Q}$  such that  $\mathbb{P}_0 = \pi_0$  and  $\mathbb{P}_T = \pi_T$ . Assume that  $\text{KL}(\mathbb{P} | \mathbb{Q}) < +\infty$ . Then  $\mathbb{P}$  is the unique Schrödinger Bridge  $\mathbb{P}^{\text{SB}}$ .*

*Proof.* The first part of the proof is a consequence of (Léonard, 2014b, Theorem 2.12(a)). The second part is a consequence of (Léonard, 2014b, Theorem 2.12(b)) and (Léonard et al., 2014, Theorem 2.14).  $\square$

### C.4 Proof of Lemma 6

**Lemma 13.** *Let  $\mathbb{M} \in \mathcal{M}$  and  $\Pi \in \mathcal{R}(\mathbb{Q})$  and assume **A1**, **A2**, **A3**. If  $\text{KL}(\Pi | \mathbb{M}) < +\infty$  and  $\text{KL}(\text{proj}_{\mathcal{M}}(\Pi) | \mathbb{M}) < +\infty$  we have*

$$\text{KL}(\Pi | \mathbb{M}) = \text{KL}(\Pi | \text{proj}_{\mathcal{M}}(\Pi)) + \text{KL}(\text{proj}_{\mathcal{M}}(\Pi) | \mathbb{M}). \quad (27)$$

*For any  $\mathbb{P} \in \mathcal{P}(\mathcal{C})$ , if  $\text{KL}(\mathbb{P} | \Pi) < +\infty$ , we have*

$$\text{KL}(\mathbb{P} | \Pi) = \text{KL}(\mathbb{P} | \text{proj}_{\mathcal{R}(\mathbb{Q})}(\mathbb{P})) + \text{KL}(\text{proj}_{\mathcal{R}(\mathbb{Q})}(\mathbb{P}) | \Pi). \quad (28)$$

*Proof.* We start with the proof of (27). Similarly to Proposition 2, where we have  $\mathbb{M} \in \mathcal{M}$  to ensure that we can apply (Léonard, 2012, Theorem 2.3), we get

$$\text{KL}(\Pi | \mathbb{M}) = \frac{1}{2} \int_0^T \mathbb{E}_{\Pi_{0,t}} [\|v_t(\mathbf{X}_t) - \sigma_t^2 \mathbb{E}_{\Pi_{T|t}}[\nabla \log \mathbb{Q}_{T|t}(\mathbf{X}_T | \mathbf{X}_t) | \mathbf{X}_0, \mathbf{X}_t]\|^2] / \sigma_t^2 dt.$$

In addition, we have

$$\text{KL}(\text{proj}_{\mathcal{M}}(\Pi) | \mathbb{M}) = \frac{1}{2} \int_0^T \mathbb{E}_{\Pi_t} [\|v_t(\mathbf{X}_t) - \sigma_t^2 \mathbb{E}_{\Pi_{T|t}}[\nabla \log \mathbb{Q}_{T|t}(\mathbf{X}_T | \mathbf{X}_t) | \mathbf{X}_t]\|^2] / \sigma_t^2 dt.$$

Finally, using Proposition 11, we have that

$$\begin{aligned} & \text{KL}(\Pi | \text{proj}_{\mathcal{M}}(\Pi)) \\ &= \frac{1}{2} \int_0^T \mathbb{E}_{\Pi_{0,t}} [\|\sigma_t^2 \mathbb{E}_{\Pi_{T|t}}[\nabla \log \mathbb{Q}(\mathbf{X}_T | \mathbf{X}_t) | \mathbf{X}_0, \mathbf{X}_t] - \sigma_t^2 \mathbb{E}_{\Pi_{T|t}}[\nabla \log \mathbb{Q}(\mathbf{X}_T | \mathbf{X}_t) | \mathbf{X}_t]\|^2] / \sigma_t^2 dt \\ &= \frac{1}{2} \int_0^T (\mathbb{E}_{\Pi_{0,t}} [\|\mathbb{E}_{\Pi_{T|t}}[\nabla \log \mathbb{Q}(\mathbf{X}_T | \mathbf{X}_t) | \mathbf{X}_0, \mathbf{X}_t]\|^2] - \mathbb{E}_{\Pi_t} [\|\mathbb{E}_{\Pi_{T|t}}[\nabla \log \mathbb{Q}(\mathbf{X}_T | \mathbf{X}_t) | \mathbf{X}_t]\|^2]) \sigma_t^2 dt. \end{aligned}$$

Using this result, we have

$$\begin{aligned} & 2\text{KL}(\Pi | \text{proj}_{\mathcal{M}}(\Pi)) + 2\text{KL}(\text{proj}_{\mathcal{M}}(\Pi) | \mathbb{M}) \\ &= \int_0^T (\mathbb{E}_{\Pi_{0,t}} [\|\mathbb{E}_{\Pi_{T|t}}[\nabla \log \mathbb{Q}(\mathbf{X}_T | \mathbf{X}_t) | \mathbf{X}_0, \mathbf{X}_t]\|^2] - \mathbb{E}_{\Pi_t} [\|\mathbb{E}_{\Pi_{T|t}}[\nabla \log \mathbb{Q}(\mathbf{X}_T | \mathbf{X}_t) | \mathbf{X}_t]\|^2]) \sigma_t^2 dt \\ &+ \int_0^T \mathbb{E}_{\Pi_t} [\|v_t(\mathbf{X}_t) / \sigma_t^2 - \mathbb{E}_{\Pi_{T|t}}[\nabla \log \mathbb{Q}_{T|t}(\mathbf{X}_T | \mathbf{X}_t) | \mathbf{X}_t]\|^2] \sigma_t^2 dt \\ &= \int_0^T (\mathbb{E}_{\Pi_{0,t}} [\|\mathbb{E}_{\Pi_{T|t}}[\nabla \log \mathbb{Q}(\mathbf{X}_T | \mathbf{X}_t) | \mathbf{X}_0, \mathbf{X}_t]\|^2] - \mathbb{E}_{\Pi_t} [\|\mathbb{E}_{\Pi_{T|t}}[\nabla \log \mathbb{Q}(\mathbf{X}_T | \mathbf{X}_t) | \mathbf{X}_t]\|^2]) \sigma_t^2 dt \\ &+ \int_0^T (\mathbb{E}_{\Pi_t} [\|v_t(\mathbf{X}_t) / \sigma_t^2\|^2] + \mathbb{E}_{\Pi_t} [\|\mathbb{E}_{\Pi_{T|t}}[\nabla \log \mathbb{Q}_{T|t}(\mathbf{X}_T | \mathbf{X}_t) | \mathbf{X}_t]\|^2]) \sigma_t^2 dt \\ &- 2 \int_0^T \mathbb{E}_{\Pi_t} [\langle v_t(\mathbf{X}_t) / \sigma_t^2, \mathbb{E}_{\Pi_{T|t}}[\nabla \log \mathbb{Q}_{T|t}(\mathbf{X}_T | \mathbf{X}_t) | \mathbf{X}_t] \rangle] \sigma_t^2 dt \\ &= \int_0^T \mathbb{E}_{\Pi_{0,t}} [\|\mathbb{E}_{\Pi_{T|t}}[\nabla \log \mathbb{Q}(\mathbf{X}_T | \mathbf{X}_t) | \mathbf{X}_0, \mathbf{X}_t]\|^2] \sigma_t^2 dt + \int_0^T \mathbb{E}_{\Pi_t} [\|v_t(\mathbf{X}_t) / \sigma_t^2\|^2] \sigma_t^2 dt \\ &- 2 \int_0^T \mathbb{E}_{\Pi_t} [\langle v_t(\mathbf{X}_t) / \sigma_t^2, \mathbb{E}_{\Pi_{T|t}}[\nabla \log \mathbb{Q}_{T|t}(\mathbf{X}_T | \mathbf{X}_t) | \mathbf{X}_t] \rangle] \sigma_t^2 dt \\ &= \int_0^T \mathbb{E}_{\Pi_{0,t}} [\|\mathbb{E}_{\Pi_{T|t}}[\nabla \log \mathbb{Q}(\mathbf{X}_T | \mathbf{X}_t) | \mathbf{X}_0, \mathbf{X}_t]\|^2] \sigma_t^2 dt + \int_0^T \mathbb{E}_{\Pi_t} [\|v_t(\mathbf{X}_t) / \sigma_t^2\|^2] \sigma_t^2 dt \\ &- 2 \int_0^T \mathbb{E}_{\Pi_{0,t}} [\langle v_t(\mathbf{X}_t) / \sigma_t^2, \mathbb{E}_{\Pi_{T|t}}[\nabla \log \mathbb{Q}_{T|t}(\mathbf{X}_T | \mathbf{X}_t) | \mathbf{X}_0, \mathbf{X}_t] \rangle] \sigma_t^2 dt = 2\text{KL}(\Pi | \mathbb{M}), \end{aligned}$$

which concludes the first part of the proof.

For (28), define  $\Pi^* = \text{proj}_{\mathcal{R}(\mathbb{Q})}(\mathbb{P}) = \int \mathbb{Q}_{|0,T} d\mathbb{P}_{0,T}$ . Using (Csiszár, 1975, Equation 2.6), we have

$$\begin{aligned} \text{KL}(\mathbb{P}|\Pi) &= \text{KL}(\mathbb{P}|\Pi^*) + \int_{\mathcal{C}} \log\left(\frac{d\Pi^*}{d\Pi}(\omega)\right) d\mathbb{P}(\omega) \\ &= \text{KL}(\mathbb{P}|\Pi^*) + \int_{\mathbb{R}^d \times \mathbb{R}^d} \log\left(\frac{d\Pi_{0,T}^*}{d\Pi_{0,T}}(x_0, x_1)\right) d\mathbb{P}_{0,T}(x_0, x_1) \\ &= \text{KL}(\mathbb{P}|\Pi^*) + \int_{\mathbb{R}^d \times \mathbb{R}^d} \log\left(\frac{d\Pi_{0,T}^*}{d\Pi_{0,T}}(x_0, x_1)\right) d\Pi_{0,T}^*(x_0, x_1) = \text{KL}(\mathbb{P}|\Pi^*) + \text{KL}(\Pi^*|\Pi), \end{aligned}$$

which concludes the proof.  $\square$

### C.5 Proof of Proposition 7

**Proposition 14.** *Assume that the conditions of Proposition 5 and Lemma 6 apply for  $\mathbb{P}^n$  for every  $n \in \mathbb{N}$  and for the Schrödinger Bridge  $\mathbb{P}^{\text{SB}}$ , we have  $\lim_{n \rightarrow +\infty} \text{KL}(\mathbb{P}^n|\mathbb{P}^{n+1}) = 0$ . If  $\mathbb{P}^*$  is a fixed point of  $(\mathbb{P}^n)_{n \in \mathbb{N}}$ , then  $\mathbb{P}^*$  is the Schrödinger Bridge.*

*Proof.* The second part of the proof is a direct application of Proposition 5, since in that case  $\mathbb{P}^*$  is Markov and reciprocal and admits  $\pi_0, \pi_T$  as marginals. For the first part of the proof, we follow the technique of Rüschemdorf (1995) but for the reverse Kullback–Leibler divergence. Applying Lemma 6, we get for any  $N \in \mathbb{N}$

$$\text{KL}(\mathbb{P}^0|\mathbb{P}^*) = \text{KL}(\mathbb{P}^0|\mathbb{P}^1) + \text{KL}(\mathbb{P}^1|\mathbb{P}^*) = \sum_{i=0}^N \text{KL}(\mathbb{P}^i|\mathbb{P}^{i+1}) + \text{KL}(\mathbb{P}^{N+1}|\mathbb{P}^*),$$

which concludes the proof.  $\square$

### C.6 Proof of Proposition 8

*Proof.* The proof is similar to the one of Proposition 2.  $\square$

In particular, the time-reversal of  $\mathbb{Q}_{|0,T}(\cdot|x_0, x_T)$  is associated with

$$d\mathbf{Y}_t^{0,T} = \{-f_{T-t}(\mathbf{Y}_t^{0,T}) + \sigma_{T-t}^2 \nabla \log \mathbb{Q}_{T-t|0}(\mathbf{Y}_t^{0,T}|x_0)\} dt + \sigma_{T-t} d\mathbf{B}_t, \quad \mathbf{Y}_0^{0,T} = x_T. \quad (29)$$

One can view both (11) (12) as SDEs with drift defined as the conditional expectation of the drift of (2) (29) under  $\Pi_{0,T|t}$  in the forward and backward directions respectively.

### C.7 Proof of Proposition 9

*Proof.* We proceed by induction. Firstly, for  $\Pi_{0,T}^0 = \mathbb{Q}_{0,T}$ ,  $\Pi^0 = \tilde{\mathbb{P}}^0 = \mathbb{Q}$  at initialization. We can also define  $\mathbb{M}^0 = \mathbb{Q}$ , such that  $\mathbb{M}^0 = \tilde{\mathbb{P}}^0$  and  $\Pi^n = \text{proj}_{\mathcal{R}(\mathbb{Q})}(\mathbb{M}^n)$  for all  $n \in \mathbb{N}$ . By (De Bortoli et al., 2021, Section 3.5), the optimal DSB sequence  $\tilde{\mathbb{P}}^n$  is Markov and  $\tilde{\mathbb{P}}^n = \int \mathbb{Q}_{|0,T} d\tilde{\mathbb{P}}_{0,T}^n$ , where  $\tilde{\mathbb{P}}_{0,T}^n$  is the IPF sequence of the static SB problem. In other words,  $\tilde{\mathbb{P}}^n \in \mathcal{M} \cap \mathcal{R}(\mathbb{Q})$ .

Suppose  $\mathbb{M}^{2n+1} = \tilde{\mathbb{P}}^{2n+1}$ . By definition,  $\mathbb{M}_0^{2n+2} = \tilde{\mathbb{P}}_0^{2n+2} = \pi_0$ , i.e. both forward processes are initialized at  $\pi_0$ . In DSB, by De Bortoli et al. (2021),  $\tilde{\mathbb{P}}^{2n+2}$  is defined as the time-reversal of  $\tilde{\mathbb{P}}^{2n+1}$ , such that  $\tilde{\mathbb{P}}_0^{2n+2} = \tilde{\mathbb{P}}_0^{2n+1}$ . Hence,  $\tilde{\mathbb{P}}^{2n+2} = \int \tilde{\mathbb{P}}_0^{2n+1} d\pi_0$ .

In DSBM, we first perform reciprocal projection  $\Pi^{2n+1} = \text{proj}_{\mathcal{R}(\mathbb{Q})}(\mathbb{M}^{2n+1}) = \int \mathbb{Q}_{|0,T} d\mathbb{M}_{0,T}^{2n+1}$ . Since  $\mathbb{M}^{2n+1} = \tilde{\mathbb{P}}^{2n+1} \in \mathcal{R}(\mathbb{Q})$ , however, we have that  $\Pi^{2n+1} = \mathbb{M}^{2n+1}$ . Furthermore, since  $\mathbb{M}^{2n+1} = \tilde{\mathbb{P}}^{2n+1} \in \mathcal{M}$ ,  $\text{proj}_{\mathcal{M}}(\Pi^{2n+1}) = \text{proj}_{\mathcal{M}}(\mathbb{M}^{2n+1}) = \mathbb{M}^{2n+1}$ . Thus,  $\mathbb{M}^{2n+2}$  given by (9) is such that  $\mathbb{M}_0^{2n+2} = \pi_0$  and  $\mathbb{M}_{|0}^{2n+2} = \text{proj}_{\mathcal{M}}(\Pi^{2n+1})_{|0} = \mathbb{M}_{|0}^{2n+1}$ . We conclude that  $\mathbb{M}^{2n+2} = \int \mathbb{M}_{|0}^{2n+1} d\pi_0 = \tilde{\mathbb{P}}^{2n+2}$ . Similar arguments holds for the the reverse projection (13). Therefore,  $\mathbb{M}^n = \tilde{\mathbb{P}}^n$  for all  $n \in \mathbb{N}$ .  $\square$

## D The set of Markov measures is not convex

Let  $p_1(x_0, x_1, x_2) = p_1(x_0)p_1(x_1|x_0)p_1(x_2|x_1)$  and  $p_2(x_0, x_1, x_2) = p_2(x_0)p_2(x_1|x_0)p_2(x_2|x_1)$  on  $\{0, 1\}^3$  such that

$$p_1(x_0 = 1) = \alpha_0, \quad p_1(x_1 = 1|x_0) = \alpha_1, \quad p_1(x_2 = 1|x_1) = \alpha_2.$$

Additionally, we set

$$p_2(x_0 = 1) = \beta_0, \quad p_2(x_1 = 1|x_0) = \beta_1, \quad p_2(x_2 = 1|x_1) = \beta_2.$$

Finally, we set  $q = (1/2)p_1 + (1/2)p_2$ . Consider  $q(x_2 = 1|x_1 = 1, x_0 = 1) = q(x_2 = 1, x_1 = 1, x_0 = 1)/q(x_1 = 1, x_0 = 1)$  and  $q(x_2 = 1|x_1 = 1) = q(x_2 = 1, x_1 = 1)/q(x_1 = 1)$ . Let

$$\begin{aligned} \Delta &= 4[q(x_2 = 1, x_1 = 1, x_0 = 1)q(x_1 = 1) - q(x_2 = 1, x_1 = 1)q(x_1 = 1, x_0 = 1)] \\ &= (\alpha_0\alpha_1\alpha_2 + \beta_0\beta_1\beta_2)(\alpha_1 + \beta_1) - (\alpha_1\alpha_2 + \beta_1\beta_2)(\alpha_0\alpha_1 + \beta_0\beta_1) \\ &= \alpha_0\alpha_1\beta_1\alpha_2 + \beta_0\alpha_1\beta_1\beta_2 - \beta_0\alpha_1\beta_1\alpha_2 - \alpha_0\alpha_1\beta_1\beta_2 \\ &= \alpha_1\beta_1\beta_2(\beta_0 - \alpha_0) + \alpha_1\beta_1\alpha_2(\alpha_0 - \beta_0) \\ &= \alpha_1\beta_1(\beta_0 - \alpha_0)(\beta_2 - \alpha_2). \end{aligned}$$

$q$  is Markov if and only if  $\Delta = 0$ . Therefore  $q$  is not Markov as soon as  $\alpha_0 \neq \beta_0$  and  $\alpha_2 \neq \beta_2$ .

## E Discrete-Time Markovian Projection

We derive in this section a discrete-time version of the Markovian projection and show that, in some limiting case, we recover the continuous-time projection. In the discrete case, we let

$$\begin{aligned} \pi(x_{0:N}) &= \pi(x_0, x_N) \prod_{k=0}^{N-1} q_{k+1|0,k,N}(x_{k+1}|x_0, x_k, x_N) \\ &= \pi(x_0, x_N) \prod_{k=0}^{N-2} q_{k+1|k,N}(x_{k+1}|x_k, x_N). \end{aligned}$$

We consider a Markovian measure  $p$  given by  $p(x_{0:N}) = p(x_0) \prod_{k=0}^{N-1} p_{k+1|k}(x_{k+1}|x_k)$ . Now let us compute  $\text{KL}(\pi|p)$ . We have

$$\begin{aligned} \text{KL}(\pi(x_{0:N})|p(x_{0:N})) &= \sum_{k=0}^{N-2} \int_{\mathbb{R}^d \times \mathbb{R}^d} \text{KL}(q_{k+1|k,N}|p_{k+1|k}) \pi_{k,N}(x_k, x_N) dx_k dx_N \\ &\quad + \text{KL}(\pi_0|p_0) + \int_{\mathbb{R}^d} \text{KL}(\pi(x_N|x_0)|p(x_N|x_{N-1})) \pi(x_0, x_{N-1}) dx_0 dx_{N-1}. \end{aligned}$$

In what follows, we denote

$$\begin{aligned} \mathcal{L}_0 &= \text{KL}(\pi_0|p_0), \quad \mathcal{L}_N = \int_{\mathbb{R}^d} \text{KL}(\pi(x_N|x_0)|p(x_N|x_{N-1})) \pi(x_0, x_{N-1}) dx_0 dx_{N-1}, \\ \mathcal{L}_{k+1} &= \int_{\mathbb{R}^d \times \mathbb{R}^d} \text{KL}(q_{k+1|k,N}|p_{k+1|k}) \pi_{k,N}(x_k, x_N) dx_k dx_N, \end{aligned}$$

We have the following proposition.

**Proposition 15.** *The minimizer  $p_{k+1|k}$  of  $\mathcal{L}_{k+1}$  is given by*

$$p_{k+1|k}(x_{k+1}|x_k) = \int_{\mathbb{R}^d} q_{k+1|k,N}(x_{k+1}|x_k, x_N) \pi_{N|k}(x_N|x_k) dx_N. \quad (30)$$

If  $p_0 = q_0$ , then for any  $k \in \{0, \dots, N-1\}$ ,  $p_k = \pi_k$ . In addition, assume that  $p_{k+1|k}(x_{k+1}|x_k) = \exp[-\|x_{k+1} - x_k - \gamma f(x_k)\|^2 / (2\gamma)] / (2\pi\gamma)^{-d/2}$  and  $q_{k+1|k,N}(x_{k+1}|x_k, x_N) = \exp[-\|x_{k+1} - x_k - \gamma f(x_k, x_N)\|^2 / (2\gamma)] / (2\pi\gamma)^{d/2}$ . Finally, assume that  $\|x_{k+1} - x_k\| \leq \gamma^{1/2}$ . Then, we have that

$$f(x_k) = \int_{\mathbb{R}^d} f(x_k, x_N) \pi(x_N|x_k) dx_N + o(\gamma^{1/2}). \quad (31)$$

*Proof.* The proofs of (30) and (31) are straightforward and left to the reader. We now prove that if  $p_0 = \pi_0$ , then for any  $k \in \{1, \dots, N\}$ ,  $p_k = \pi_k$ . First, we have that for any  $k \in \{0, \dots, N-1\}$ ,

$$\pi(x_k, x_{k+1}, x_N) = \pi(x_k, x_N) q(x_{k+1}|x_k, x_N).$$

Assume now that  $p_k = \pi_k$ , then we have

$$\begin{aligned} p_{k+1}(x_{k+1}) &= \int_{\mathbb{R}^d} p_k(x_k) p_{k+1|k}(x_{k+1}|x_k) dx_k \\ &= \int_{\mathbb{R}^d \times \mathbb{R}^d} p_k(x_k) q_{k+1|k,N}(x_{k+1}|x_k, x_N) \pi_{N|k}(x_N|x_k) dx_k dx_N \\ &= \int_{\mathbb{R}^d \times \mathbb{R}^d} \pi_k(x_k) q_{k+1|k,N}(x_{k+1}|x_k, x_N) \pi_{N|k}(x_N|x_k) dx_k dx_N \\ &= \int_{\mathbb{R}^d \times \mathbb{R}^d} \pi_{k,k+1,N}(x_k, x_{k+1}, x_N) dx_k dx_N = \pi_{k+1}(x_{k+1}), \end{aligned}$$

which concludes the proof.  $\square$



In particular, in the previous proposition, if  $f(x_k, x_N) = \nabla \log q(x_N | x_k)$ , i.e. we have a discretization of the bridge then  $f(x_k) = \int_{\mathbb{R}^d} \nabla \log q(x_N | x_k) \pi(x_N | x_k) dx_N$ , which recovers the Markovian projection in continuous-time.

## F Comparing DSBM-IPF and DSB

We analyze further the differences between DSBM-IPF proposed here and DSB proposed in [De Bortoli et al. \(2021\)](#). Both algorithms solve the SB problem using the IPF iterates. Algorithmically, the difference occurs in the trajectory caching step. In DSB, a fixed discretization of SDE needs to be chosen, and all intermediate samples from the discretized Euler-Maruyama simulation of the SDE need to be saved. Furthermore, a second set of drift evaluation needs to be performed for all datapoints in the trajectory ([De Bortoli et al., 2021](#), Equations (12), (13)). On the contrary, DSBM-IPF discards all intermediate samples during trajectory caching and only retains the joint samples at times  $0, T$ . Then, the intermediate trajectories are reconstructed using the reference bridge  $\mathbb{Q}_{|0,T}$ .

In addition to the benefits of continuous-time training of SB and lower computational and memory costs than DSB as discussed in the main text, we investigate here further the benefit of explicitly projecting onto the reciprocal class of  $\mathbb{Q}$ . Intuitively speaking, we directly incorporate the reference measure  $\mathbb{Q}$  in the training procedure as our inductive bias. More formally, suppose we have at the current IPF iteration  $\mathbb{M}^{2n}$  (Markov diffusion in the forward direction) and want to learn  $\mathbb{M}^{2n+1}$  (Markov diffusion in the backward direction). Due to training error accumulating, however,  $\mathbb{M}^{2n}$  no longer has the correct bridge  $\mathbb{Q}_{|0,T}$ . Now suppose we first perform IMF for  $\mathbb{M}^{2n}$  and learn  $\mathbb{M}^{2n,*}$  in the forward direction. That is to say, we repeat alternative reciprocal and Markovian projections and obtain a sequence  $(\mathbb{M}^{2n,m})_{m \in \mathbb{N}}$  in the forward direction converging to  $\mathbb{M}^{2n,*}$ . Then  $\mathbb{M}^{2n,*}$  now has the correct bridge  $\mathbb{Q}_{|0,T}$  by Proposition 7, since  $\mathbb{M}^{2n,*}$  is the SB between  $\mathbb{M}_0^{2n}$  and  $\mathbb{M}_T^{2n}$ . Theoretically,  $\mathbb{M}_t^{2n} = \mathbb{M}_t^{2n,*}$  for  $t = 0, T$ , but due to training error accumulating it may be that  $\mathbb{M}_T^{2n} \neq \mathbb{M}_T^{2n,*}$ . However,  $\mathbb{M}_0^{2n} = \mathbb{M}_0^{2n,*}$ , since  $\mathbb{M}^{2n,*}$  is in the forward direction and starting from samples from  $\pi_0$ . As a result, we can obtain a Markov forward diffusion  $\mathbb{M}^{2n,*}$ , which has  $\mathbb{M}_0^{2n,*} = \pi_0$  and the correct bridge  $\mathbb{Q}_{|0,T}$ . These are the same set of properties that the reference measure  $\mathbb{Q}$  has. As a result, replacing  $\mathbb{Q}$  with  $\mathbb{M}^{2n,*}$  in (6) results in the same SB solution. Consequently, now continuing the IPF iterations from  $\mathbb{M}_0^{2n,*}$ , it is as if we restart IPF afresh using a modified SB problem

$$\mathbb{P}^{\text{SB}} = \operatorname{argmin}\{\text{KL}(\mathbb{P} | \mathbb{M}^{2n,*}) : \mathbb{P}_0 = \pi_0, \mathbb{P}_T = \pi_T\}.$$

If  $\mathbb{M}^{2n,*}$  is closer than  $\mathbb{Q}$  to  $\mathbb{M}^*$  in the sense of KL divergence, then we obtain a better initialization of the IPF procedure.

As proposed in Algorithm 1, DSBM performs the Markovian and reciprocal projection only once before switching between the forward and backward directions. However, it is still beneficial compared to DSB with less bias accumulation in the bridge.

## G Joint Training of Forward and Backward Processes

We recall below the DSBM algorithm given in Algorithm 1.

---

### Algorithm 2 Diffusion Schrödinger Bridge Matching

---

- 1: **Input:** Joint distribution  $\Pi_{0,T}^0$ , tractable bridge  $\mathbb{Q}_{|0,T}$ , number of outer iterations  $N \in \mathbb{N}$ .
  - 2: Let  $\Pi^0 = \int \mathbb{Q}_{|0,T} d\Pi_{0,T}^0$ .
  - 3: **for**  $n \in \{0, \dots, N-1\}$  **do**
  - 4:   Learn  $v_{\phi^*}$  using (14) with  $\Pi = \Pi^{2n}$ .
  - 5:   Let  $\mathbb{M}^{2n+1}$  be given by (13).
  - 6:   Let  $\Pi^{2n+1} = \int \mathbb{Q}_{|0,T} d\mathbb{M}_{0,T}^{2n+1}$ .
  - 7:   Learn  $v_{\theta^*}$  using (10) with  $\Pi = \Pi^{2n+1}$ .
  - 8:   Let  $\mathbb{M}^{2n+2}$  be given by (9).
  - 9:   Let  $\Pi^{2n+2} = \int \mathbb{Q}_{|0,T} d\mathbb{M}_{0,T}^{2n+2}$ .
  - 10: **end for**
  - 11: **Output:**  $v_{\theta^*}, v_{\phi^*}$
-

Our main observation comes from Proposition 8. In particular, under mild assumptions, we have that the Markovian projection  $\mathbb{M} = \text{proj}_{\mathcal{M}}(\Pi)$  is associated with

$$\begin{aligned} d\mathbf{X}_t &= \{f_t(\mathbf{X}_t) + \sigma_t^2 \mathbb{E}_{\Pi_{T|t}}[\nabla \log \mathbb{Q}_{T|t}(\mathbf{X}_T | \mathbf{X}_t) | \mathbf{X}_t]\}dt + \sigma_t d\mathbf{B}_t, \quad \mathbf{X}_0 \sim \pi_0, \\ d\mathbf{Y}_t &= \{-f_{T-t}(\mathbf{Y}_t) + \sigma_{T-t}^2 \mathbb{E}_{\Pi_{0|T-t}}[\nabla \log \mathbb{Q}_{T-t|0}(\mathbf{Y}_T | \mathbf{Y}_t) | \mathbf{Y}_t]\}dt + \sigma_{T-t} d\mathbf{B}_t, \quad \mathbf{Y}_0 \sim \pi_T. \end{aligned}$$

Considering the following losses,

$$\theta^* = \text{argmin}_{\theta} \left\{ \int_0^T \mathbb{E}_{\Pi_{t,T}} [\|\sigma_t^2 \nabla \log \mathbb{Q}_{T|t}(\mathbf{X}_T | \mathbf{X}_t) - v_{\theta}(t, \mathbf{X}_t)\|^2] / \sigma_t^2 dt : \theta \in \Theta \right\}, \quad (32)$$

$$\phi^* = \text{argmin}_{\phi} \left\{ \int_0^T \mathbb{E}_{\Pi_{t,0}} [\|\sigma_t^2 \nabla \log \mathbb{Q}_{t|0}(\mathbf{X}_t | \mathbf{X}_0) - v_{\phi}(t, \mathbf{X}_t)\|^2] / \sigma_t^2 dt : \phi \in \Phi \right\}. \quad (33)$$

If the families of functions  $\{v_{\theta} : \theta \in \Theta\}$  and  $\{v_{\phi} : \theta \in \Phi\}$  are rich enough, we have for any  $t \in [0, T]$  and  $x_t \in \mathbb{R}^d$ ,  $v_{\theta^*}(t, x_t) = \sigma_t^2 \mathbb{E}_{\Pi_{T|t}}[\nabla \log \mathbb{Q}_{T|t}(\mathbf{X}_T | \mathbf{X}_t) | \mathbf{X}_t = x_t]$  and  $v_{\phi^*}(t, x_t) = \sigma_t^2 \mathbb{E}_{\Pi_{0|t}}[\nabla \log \mathbb{Q}_{t|0}(\mathbf{X}_t | \mathbf{X}_0) | \mathbf{X}_t = x_t]$ . In practice, this means that the Markovian projection can be computed in a forward *or* backward fashion equivalently.

Therefore, given a coupling  $\Pi = \Pi^{2n}$ , we can update *both*  $v_{\theta}$  and  $v_{\phi}$ . This means that we train the forward and backward model *jointly*. We then consider  $\mathbb{M}_b^{2n+1}$  associated with (13) and  $\mathbb{M}_f^{2n+1}$  associated with (9). Note that if the families of functions  $\{v_{\theta} : \theta \in \Theta\}$  and  $\{v_{\phi} : \theta \in \Phi\}$  are rich enough then  $\mathbb{M}_f^{2n+1} = \mathbb{M}_b^{2n+1}$ .

**Mixture from forward and backward.** Once we have obtained both the forward update and the backward update, our next task is to define the new mixture of bridge  $\Pi^{2n+1}$ . In Algorithm 1, since we train only the *backward* model  $\mathbb{M}^{2n+1} = \mathbb{M}_b^{2n+1}$ , we define  $\Pi^{2n+1} = \int \mathbb{Q}_{|0,T} d\mathbb{M}_{0,T}^{2n+1}$ . In the case of *joint training*, we have access to  $\mathbb{M}_b^{2n+1}$  and  $\mathbb{M}_f^{2n+1}$ . One way to define a new mixture of bridge is to compute  $\Pi^{2n+1} = \frac{1}{2}(\int \mathbb{Q}_{|0,T} d\mathbb{M}_{b,0,T}^{2n+1} + \int \mathbb{Q}_{|0,T} d\mathbb{M}_{f,0,T}^{2n+1})$ . This choice ensures that in the case where  $\mathbb{M}_f^{2n+1} = \mathbb{M}_b^{2n+1}$  we have

$$\Pi^{2n+1} = \int \mathbb{Q}_{|0,T} d\mathbb{M}_{f,0,T}^{2n+1} = \int \mathbb{Q}_{|0,T} d\mathbb{M}_{b,0,T}^{2n+1}.$$

It also ensures that all the steps in the *joint* DSBM training algorithms are symmetric. We leave the study of an optimal combination of  $\mathbb{M}_f^{2n+1}$  and  $\mathbb{M}_b^{2n+1}$  for future work.

**Consistency loss.** In addition to the losses (32) and (33), we also consider an additional *consistency* loss. A similar idea was explored in Song (2022). In DSB (De Bortoli et al., 2021; Chen et al., 2022) and DSBM, see Algorithm 1, the processes parameterized by  $v_{\theta}$  (forward) and  $v_{\phi}$  backward are identical *only at equilibrium*. Thus imposing the forward and the backward processes match at each step of DSB or DSBM would lead to some bias. However, this is not the case in the *joint training* setting. Indeed, in that case, we have  $\mathbb{M}_f^{2n+1} = \mathbb{M}_b^{2n+1}$  if the families are rich enough. Therefore, we get that

$$d\mathbf{Y}_t = \{-f_{T-t}(\mathbf{Y}_t) + v_{\phi}(T-t, \mathbf{Y}_t)\}dt + \sigma_{T-t} d\mathbf{B}_t, \quad \mathbf{Y}_0 \sim \pi_T, \quad (34)$$

is the time reversal of

$$d\mathbf{X}_t = \{f_t(\mathbf{X}_t) + v_{\theta}(t, \mathbf{X}_t)\}dt + \sigma_t d\mathbf{B}_t, \quad \mathbf{X}_0 \sim \pi_0. \quad (35)$$

Computing the time-reversal of (34), we have

$$d\mathbf{X}_t = \{f_t(\mathbf{X}_t) - v_{\phi}(t, \mathbf{X}_t) + \sigma_t^2 \nabla \log \Pi_t^{2n}(\mathbf{X}_t)\}dt + \sigma_t d\mathbf{B}_t, \quad \mathbf{X}_0 \sim \pi_0. \quad (36)$$

Identifying (36) and (35), we get that for any  $t \in [0, T]$  and  $x_t \in \mathbb{R}^d$

$$v_{\theta}(t, x_t) = -v_{\phi}(t, x_t) + \sigma_t^2 \nabla \log \Pi_t^{2n}(x_t).$$

We highlight that letting  $\sigma_t \rightarrow 0$  for any  $t \in [0, T]$ , we get that  $v_{\theta} = -v_{\phi}$ , which confirms that the time-reversal of an ODE is simply given by flipping the sign of the velocity. Therefore, we propose the following loss which links the parameters  $\theta$  and  $\phi$

$$\mathcal{L}_{\text{cons}}(\theta, \phi) = \int_0^T \mathbb{E}_{\Pi_t^{2n}} [\|v_{\theta}(t, \mathbf{X}_t) + v_{\phi}(t, \mathbf{X}_t) - \sigma_t^2 \nabla \log \Pi_t^{2n}(\mathbf{X}_t)\|^2] / \sigma_t^2 dt.$$

Leveraging tools from score matching (Hyvärinen, 2005) and the divergence theorem, we get that

$$\mathcal{L}_{\text{cons}}(\theta, \phi) = \int_0^T \mathbb{E}_{\Pi_t^{2n}} [\|v_\theta(t, \mathbf{X}_t) + v_\phi(t, \mathbf{X}_t)\|^2 / \sigma_t^2 + 2\text{div}(v_\theta(t, \mathbf{X}_t) + v_\phi(t, \mathbf{X}_t))] dt + C,$$

where  $C \geq 0$  is a constant which does not depend on  $\theta$  and  $\phi$ . Below, we recall the two losses used to estimate the Markovian projection (32) and (33)

$$\begin{aligned} \mathcal{L}(\theta) &= \int_0^T \mathbb{E}_{\Pi_{t,T}} [\|\sigma_t^2 \nabla \log \mathbb{Q}_{T|t}(\mathbf{X}_T | \mathbf{X}_t) - v_\theta(t, \mathbf{X}_t)\|^2] / \sigma_t^2 dt, \\ \mathcal{L}(\phi) &= \int_0^T \mathbb{E}_{\Pi_{t,0}} [\|\sigma_t^2 \nabla \log \mathbb{Q}_{t|0}(\mathbf{X}_t | \mathbf{X}_0) - v_\phi(t, \mathbf{X}_t)\|^2] / \sigma_t^2 dt. \end{aligned}$$

The complete loss we consider in the joint training of the algorithm is of the form

$$\mathcal{L}_\lambda(\theta, \phi) = \mathcal{L}(\theta) + \mathcal{L}(\phi) + \lambda \mathcal{L}_{\text{cons}}(\theta, \phi), \quad (37)$$

where  $\lambda > 0$  is an additional regularization parameter. We are now ready to state the full *joint training* version of DSBM, in Algorithm 3.

---

**Algorithm 3** Diffusion Schrödinger Bridge Matching (Joint Training)

---

- 1: **Input:** Coupling  $\Pi_{0,T}^0$ , tractable bridge  $\mathbb{Q}_{|0,T}$ ,  $N \in \mathbb{N}$
  - 2: Let  $\Pi^0 = \int \mathbb{Q}_{|0,T} d\Pi_{0,T}^0$ .
  - 3: **for**  $n \in \{0, \dots, N-1\}$  **do**
  - 4:   Learn  $v_{\phi^*}, v_{\theta^*}$  using (37) with  $\Pi = \Pi^n$ .
  - 5:   Let  $\mathbb{M}_f^{n+1}$  be given by (9).
  - 6:   Let  $\mathbb{M}_b^{n+1}$  be given by (13).
  - 7:   Let  $\mathbb{M}^{n+1} = \frac{1}{2}(\mathbb{M}_f^{n+1} + \mathbb{M}_b^{n+1})$ .
  - 8:   Let  $\Pi^{n+1} = \int \mathbb{Q}_{|0,T} d\mathbb{M}_{0,T}^{n+1}$ .
  - 9: **end for**
  - 10: **Output:**  $v_{\theta^*}, v_{\phi^*}$
- 

## H Loss Scaling

Similar to the loss weighting in standard diffusion models (Song et al., 2021b; Ho et al., 2020), we derive a similar weighting to reduce the variance of our objective. We focus on the forward direction of Markovian projection in this case, and the backward case can be derived similarly. Our forward loss in the DSBM framework is given by (10), where the inner expectation is given by

$$\mathbb{E}_{\Pi_{t,T}} [\|\sigma_t^2 \nabla \log \mathbb{Q}_{T|t}(\mathbf{X}_T | \mathbf{X}_t) - v_\theta(t, \mathbf{X}_t)\|^2].$$

Letting  $\mathbb{Q}_{|0,T}$  be a Brownian bridge with diffusion parameter  $\sigma$  and assuming  $T = 1$ , this becomes

$$\mathbb{E}_{(\mathbf{X}_0, \mathbf{X}_1) \sim \Pi_{0,1}, \mathbf{Z} \sim \mathcal{N}(0, \text{Id})} [\|\mathbf{X}_1 - \mathbf{X}_0 - \sigma \sqrt{t/(1-t)} \mathbf{Z} - v_\theta(t, \mathbf{X}_t^{0,T})\|^2]$$

with  $\mathbf{X}_t^{0,T} = t\mathbf{X}_1 + (1-t)\mathbf{X}_0 + \sigma \sqrt{t(1-t)} \mathbf{Z}$ . When  $t \approx 1$ , we see that the regression target is dominated by the noise term  $\sigma \sqrt{t/(1-t)} \mathbf{Z}$  which needs to be predicted based on information contained within  $\mathbf{X}_t^{0,T}$ . The loss will have an approximate scale of  $\sigma^2 t / (1-t)$  when  $t \approx 1$  which will be very large. To avoid these large values affecting gradient descent, we can downweight the loss by  $1 + \sigma^2 t / (1-t)$  (we can add 1 to effectively cause no loss scaling when  $t$  is close to 0).

$$(1 + \sigma^2 t / (1-t))^{-1} \mathbb{E}_{(\mathbf{X}_0, \mathbf{X}_1) \sim \Pi_{0,1}, \mathbf{Z} \sim \mathcal{N}(0, \text{Id})} [\|\mathbf{X}_1 - \mathbf{X}_0 - \sigma \sqrt{t/(1-t)} \mathbf{Z} - v_\theta(t, \mathbf{X}_t^{0,T})\|^2].$$

Similar arguments can be applied to the backward loss (14)

$$\begin{aligned} &\mathbb{E}_{\Pi_{t,0}} [\|\sigma_t^2 \nabla \log \mathbb{Q}_{t|0}(\mathbf{X}_t | \mathbf{X}_0) - v_\phi(t, \mathbf{X}_t)\|^2] \\ &= \mathbb{E}_{(\mathbf{X}_0, \mathbf{X}_1) \sim \Pi_{0,1}, \mathbf{Z} \sim \mathcal{N}(0, \text{Id})} [\|\mathbf{X}_0 - \mathbf{X}_1 - \sigma \sqrt{(1-t)/t} \mathbf{Z} - v_\phi(t, \mathbf{X}_t^{0,T})\|^2], \end{aligned}$$

which we then downweight by  $1 + \sigma^2(1-t)/t$

$$(1 + \sigma^2(1-t)/t)^{-1} \mathbb{E}_{(\mathbf{X}_0, \mathbf{X}_1) \sim \Pi_{0,1}, \mathbf{Z} \sim \mathcal{N}(0, \text{Id})} [\|\mathbf{X}_0 - \mathbf{X}_1 - \sigma \sqrt{(1-t)/t} \mathbf{Z} - v_\phi(t, \mathbf{X}_t^{0,T})\|^2].$$

## I Experiment Details

In this section, we present further details of the experiment setups as well as further experiment results. In all experiments, we use Brownian motion for the reference measure  $\mathbb{Q}$  with corresponding Brownian bridge (3), the Adam optimizer with learning rate  $10^{-4}$ , SiLU activation, and  $T = 1$ .

### I.1 2D Experiments

For the 2D experiments, we follow [Tong et al. \(2023\)](#) closely and use the same datasets and 2-Wasserstein distance between the test set and samples simulated using probability flow ODE as the evaluation metric. However, we use 10000 samples in the test set since we find the 2-Wasserstein distance can vary greatly with only 1000 samples (which can be as high as 0.3 even between two set of samples both drawn from the ground truth distribution). We use a simple MLP with 3 hidden layers and 256 hidden units to parameterize the forward and backward drift networks. We use batch size 128 and 20 diffusion steps. Each outer iteration is trained for 10000 steps and we train for 20 outer iterations. For flow methods, we train for 200000 steps in total. For [Table 2](#) we use  $\sigma_t = 1$  in all cases, except the moons-8gaussians dataset where we use  $\sigma_t = 5$ .

### I.2 Gaussian Experiment

Similar to the 2D experiments, we use a simple MLP with 2 hidden layers and 256 hidden units to parameterize the forward and backward drift networks. This is a smaller network compared to the “large” network in [De Bortoli et al. \(2021\)](#). We use batch size 128 and 20 diffusion steps. Each outer iteration is trained for 10000 steps and we train for 20 outer iterations.

For [Table 4](#), we assume the marginals of the learned process  $\mathbb{P}_t$  are also independently Gaussian distributed in each dimension. We thus estimate the KL divergence using the sample mean and variance of each dimension of  $\mathbb{P}_t$  and the analytic KL expression between Gaussian distributions.

### I.3 Image Experiment

We follow [De Bortoli et al. \(2021\)](#) closely for the setup of this experiment. We use the same U-Net architecture, batch size 128 and 30 diffusion steps. Each outer iteration is trained for 5000 steps. We train for at most 50 outer iterations (i.e. 250000 total number of steps).

Contrary to [De Bortoli et al. \(2021\)](#), in our experiments we find that we can improve the sampling quality of both DSB and DSBM by choosing a uniform noising schedule. We simply choose  $\sigma_t = 1$  for all  $t$  and  $T = 1$  in our experiments.

We provide further experiment results in [Figures 7, 8 and 9](#). In [Figure 7](#), we show samples generated using different algorithms and at different points of convergence. Samples generated using CFM and 2-Rectified Flow with 2 rectified steps in (a) and (b) appear to be less clear and identifiable. OT-CFM improves upon CFM slightly in (c), but many samples still appear to be unclear. For DSB, the algorithm has not converged after 10 iterations, and many samples in (d) still appear to be letters. After 20 iterations, there are still letter-like samples, in particular many ‘C’ in [Figure 5b](#), and the digit classes also appear to be unbalanced with many instances of digit ‘0’. After 30 iterations, however, the sample quality of DSB becomes very poor in (e). On the other hand, as shown in (f)-(j), we observe that DSBM converges faster than DSB, with more accurate samples even in iterations 10 and 20. At the end of training, DSBM generates samples of highest quality after 50 iterations.

We present some additional trajectory samples at the end of training using DSBM in [Figures 8 and 9](#) in both the forward and backward directions. We observe DSBM is able to transfer samples across the two domains faithfully, and the output samples preserve interesting similarities compared to the input.

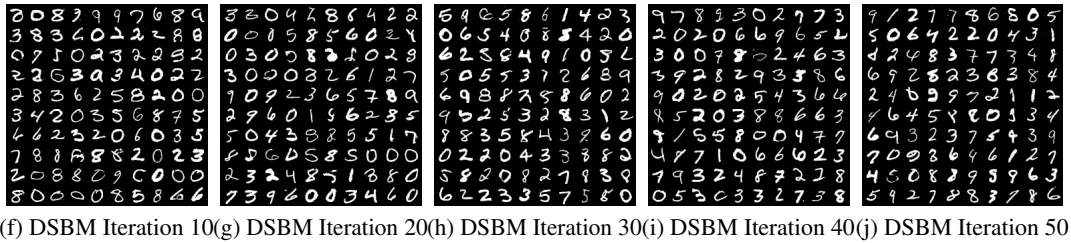
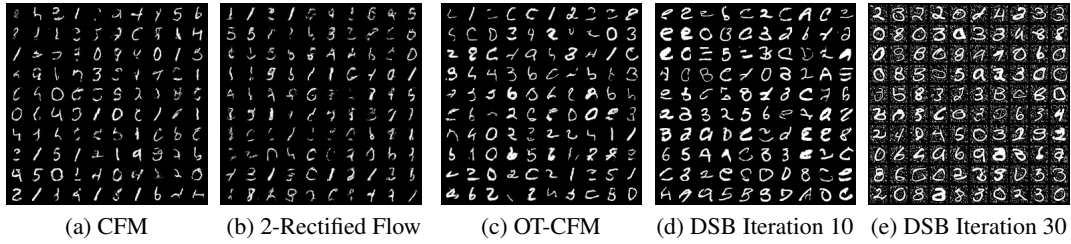


Figure 7: Samples of MNIST digits transferred from the EMNIST letters using different methods.

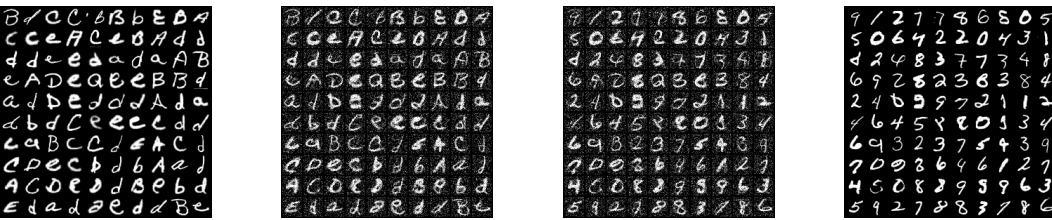


Figure 8: EMNIST to MNIST sample trajectory of DSBM with 30 diffusion steps at iteration 50 and  $t = 0, 1/3, 2/3, 1$ .

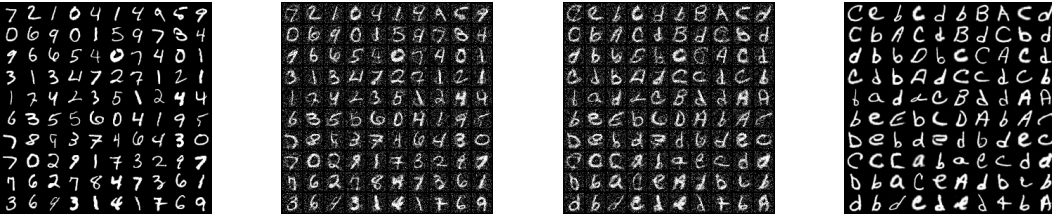


Figure 9: MNIST to EMNIST sample trajectory of DSBM with 30 diffusion steps at iteration 50 and  $t = 0, 1/3, 2/3, 1$ .